

NUCLEAR RADIATION SHIELDING STUDIES

Report No. 6



6169130

MONTE CARLO CALCULATION OF THE SPECTRUM OF GAMMA RADIATION FROM A COLLIMATED CO-60 SOURCE

By

E. E. MORRIS AND A. B. CHILTON

A FINAL REPORT OF AN INVESTIGATION CONDUCTED
under the sponsorship of
THE OFFICE OF CIVIL DEFENSE
under
Contract N0022866C0311
OCD Work Unit 1112C

UNIVERSITY OF ILLINOIS
URBANA, ILLINOIS

DECEMBER 1967

THIS DOCUMENT HAS BEEN APPROVED
FOR PUBLIC RELEASE AND SALE.
DISTRIBUTION IS UNLIMITED.

by
CLEARING HOUSE

■ ■ ■

DISCLAIMER NOTICE

**THIS DOCUMENT IS BEST QUALITY
PRACTICABLE. THE COPY FURNISHED
TO DTIC CONTAINED A SIGNIFICANT
NUMBER OF PAGES WHICH DO NOT
REPRODUCE LEGIBLY.**

AD 669 120

MONTE CARLO CALCULATION OF THE SPECTRUM OF
GAMMA RADIATION FROM A COLLIMATED CO-60 SOURCE

E.E. Morris, et al

Illinois University
Urbana, Illinois

December 1967

MONTE CARLO CALCULATION OF THE SPECTRUM OF GAMMA RADIATION
FROM A COLLIMATED Co-60 SOURCE

by

E. E. Morris and A. B. Chilton

University of Illinois

Nuclear Radiation Shielding Studies

Report No. 6

December 1967

NRDL TRC-68-6

for

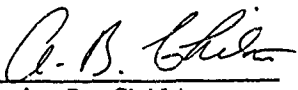
Office of Civil Defense
Office of the Secretary of the Army
Washington, D. C. 20310

through the

U. S. Naval Radiological Defense Laboratory
San Francisco, California 94135

Contract N0022866C0311; OCD Work Unit 1112C

Approved:


A. B. Chilton
Principal Investigator

OCD Review Notice

This report has been reviewed in the Office of Civil Defense and approved for publication. Approval does not signify that the contents necessarily reflect the views and policies of the Office of Civil Defense.

This document has been approved for public release and sale;
its distribution is unlimited.

SUMMARY

This report gives the results of a Monte Carlo calculation of the energy spectrum and angular distribution of gamma radiation emitted by a collimated cobalt-60 source. It is an extension of a previous report from the University of Illinois (K. Preiss, "Monte Carlo Calculation of Self Shielding by Encapsulated Gamma Ray Sources," Univ. of Ill. Rpt. NRSS-3, August 1966).

The program developed is flexible enough to give results for a wide variety of geometric situations of source container and collimator; however, the results of the specific calculation are for the particular one used by the University of Illinois in its shielding experimentation. Minor simplifications in the precise geometry have been made for ease of programming, but such simplifications are not of a nature to change the results to any appreciable extent.

In the Monte Carlo calculation, the major simplification in technique involves the use of a fictitious interaction to facilitate the handling of some of the boundary problems. In essence, if this interaction is properly introduced, two media having tabulated attenuation coefficients which are slightly different can be made to have the same total interaction coefficient for the purpose of calculating path lengths, and the points of boundary crossing between these two media need not be calculated. (This technique seems to have been first mentioned by Woodcock et al., U.S. AEC Rpt. TID 4500, May 1965.)

The output data are given in terms of 13 energy groups, from 1.4 MeV down to 0.1 MeV, and 3 angle groups. The angle groups involve: first, a narrow cone in which all radiation passing through the collimator without interaction must be included; a somewhat wider cone which is established by a secondary collimator placed on top the first to minimize lip scatter problems; and the remainder which includes all lip scatter out to 90° from the axis of the collimator. The first angular group contains about 80% of the emergent photons and the other two groups contain about 10% each.

For the spectrum in the first angular interval, scattered photons constitute 16%. The low energy spectrum rises to a peak in the energy

interval 0.2 to 0.3 MeV. The peak results primarily from the fact that the single-scattering cutoff energies for both source energies lie in this interval. The spectrum results almost entirely from scatterings in the source and its capsule, with very little contribution from collimator scatterings.

The results are in qualitative agreement with previous calculations published by Cormack and Johns for a somewhat similar situation (British Journal of Radiology, 31, No. 369, 497, 1958). Agreement is also good with experimental measurements of Costrell on encapsulated sources (Health Physics, 8, 261, 1962), except at very low energies.

Modifications of the emergent spectrum by introduction of lead filter plates across the collimator are included.

MONTE CARLO CALCULATION OF THE SPECTRUM OF GAMMA RADIATION
FROM A COLLIMATED Co-60 SOURCE

by

E. E. Morris and A. B. Chilton
University of Illinois
Nuclear Radiation Shielding Studies

Report No. 6

December 1967

NRDL TRC-68-6

for

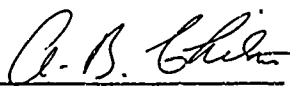
Office of Civil Defense
Office of the Secretary of the Army
Washington, D. C. 20310

through the

U. S. Naval Radiological Defense Laboratory
San Francisco, California 94135

Contract N0022866C0311; OCD Work Unit 1112C

Approved:


A. B. Chilton
Principal Investigator

GCD Review Notice

This report has been reviewed in the Office of Civil Defense and approved for publication. Approval does not signify that the contents necessarily reflect the views and policies of the Office of Civil Defense.

This document has been approved for public release and sale; its distribution is unlimited.

ACKNOWLEDGEMENT

Assistance provided by Mr. Riaz Khadem in the early stages of this work is gratefully acknowledged. Also, appreciation is expressed to Dr. K. Preiss for reading the manuscript of the report and his constructive comments on it.

ABSTRACT

A Monte Carlo calculation of the energy spectrum emitted by a collimated, Co-60 source is reported. The collimator assumed is very similar to one currently being used in experimental shielding studies at the University of Illinois. Radiation emerging from the collimator is classified into 13 equal-length energy intervals between 0.1 and 1.4 MeV , and into 3 direction intervals for angles relative to the collimator axis between 0° and 90° . Comparisons are made with experimental and theoretical work reported by others.

TABLE OF CONTENTS

	Page
I. INTRODUCTION	1
II. DESCRIPTION OF THE CALCULATIONAL BASIS OF THE MONTE CARLO PROGRAM	2
III. RESULTS AND COMPARISON WITH OTHER WORK	6
IV. CONCLUSION	10
REFERENCES	11
FIGURES	12
APPENDIX A FILTERED SPECTRA	19
APPENDIX B MASS ATTENUATION COEFFICIENTS	22
APPENDIX C DESCRIPTION OF FORTRAN PROGRAM CØLLIMATØR	24
C.1 GENERAL REMARKS	24
C.2 DESCRIPTION OF INDIVIDUAL SUBROUTINES	25
C.3 PROGRAM LISTINGS AND SAMPLE OUTPUT	32

I. INTRODUCTION

This report gives the results of a Monte Carlo calculation of the energy spectrum and angular distribution of gamma radiation emitted by a collimated Co-60 source. It is an extension of earlier work reported by Preiss⁽¹⁾ for uncollimated, encapsulated sources.

Preiss cites several instances where discrepancies between theoretical calculations and corresponding experimental results have been traced to neglect of source spectrum degradation due to scattering either in the source material or in material near the source. The spectra in this report are to be used as input for calculations of gamma-ray penetration through ribbed slabs. The results of these calculations in turn will be compared with results of experimental studies of ribbed-slab shielding properties being conducted at the University of Illinois.

The collimated source for which the present calculation was made is shown in Figure 1. The source being used in the experimental work mentioned above differs from the collimated source in Figure 1 in that the experimental source capsule is held in place by a collar made of Firth Heavy Metal. This alloy consists of about 90% tungsten with the remaining 10% consisting of copper and nickel. In Figure 1, the collar is regarded as "black." The approximation thus made is not expected to have a significant influence on the usefulness of the calculated results.

The Monte Carlo calculation on which the data in this report are based is described in Section II. The mass attenuation coefficients used in the calculation are given in Appendix B along with a description of the procedure employed to evaluate interaction coefficients for cobalt. The computer program for the Monte Carlo calculation is described in Appendix C.

Some experimental measurements of spectra from collimated Co-60 sources have been reported.^(2,3,4) Among these, one of the sources considered by Costrell⁽²⁾ corresponds fairly closely to the collimated source in Figure 1. We compare with one of his spectra in Section III. Also in Section III, our results are compared with the Monte Carlo work of Preiss⁽¹⁾ and with a calculation by Cormack and Johns.⁽⁵⁾

Frequently, in order to reduce the importance of low energy scattered radiation relative to primary radiation, the source spectrum is filtered by placing a thin sheet of lead between the source and the target. In Appendix A, spectra which have been filtered in this way are presented for lead thicknesses of 1/8 and 1/4 inch.

II. DESCRIPTION OF THE CALCULATIONAL BASIS OF THE MONTE CARLO PROGRAM

The axis of the collimator was taken as the Z-axis of a cartesian coordinate system. Photon positions were then given in terms of rectangular coordinates and photon directions were specified by direction cosines relative to each of the coordinate axes.

The Co-60 was assumed to be uniformly distributed in the cobalt metal (Figure 1). At the beginning of the calculation, a finite set of source points which were assumed to represent the uniform distribution were selected. The selection was made by dividing the source region into a number of equal volume increments and picking a single source point in each increment. Because of cylindrical symmetry, the volume increments were chosen in the shape of annuli. They were defined by dividing the source region into a number of equal thickness layers all parallel to the plane $z = 0$, and then further dividing each layer into several concentric rings. The source point for a particular volume increment was selected so that it was located on the XZ-plane with $x > 0$, halfway between the top and bottom planes, and halfway between the inner and outer radii of the volume. As the calculation progressed, source points were then systematically selected from this predetermined list so that for each of the source energies 1.17 and 1.33 MeV, the same number of photon histories originated at each source point.

Initial photon directions were sampled randomly from an isotropic distribution.

The basic interaction considered in the calculation other than absorption was Compton scattering. Absorption was taken primarily as photoelectric; but for the short energy interval 1.022 to 1.33 MeV, the pair production interaction was also treated as absorptive.

In addition, we followed the procedure first reported by Woodcock, et al.⁽⁶⁾ and subsequently used by Preiss,⁽¹⁾ of introducing a fictitious

interaction to facilitate the handling of some of the boundary problems. This procedure may be described as follows: Consider two media with an interface between them. Let μ_1 and μ_2 be the linear attenuation coefficients for medium 1 and medium 2 respectively. Further, suppose $\mu_2 > \mu_1$. If a photon interacts in medium 2 and is not absorbed, then we sample a path length to the next interaction point using the equation,

$$s = -\frac{1}{\mu_2} \ln \rho ,$$

where s is the path length and ρ is a random number between 0 and 1. If the path carries the photon across the interface into medium 1, we write,

$$\mu_2 = (\mu_2 - \mu_1) + \mu_{a1} + \mu_{s1} ,$$

where

$$\mu_1 = \mu_{a1} + \mu_{s1} ,$$

and where μ_{a1} and μ_{s1} are the linear absorption and scattering coefficients for medium 1. Three possible interactions are then considered instead of the usual two. The first, with probability

$$\frac{\mu_2 - \mu_1}{\mu_2} ,$$

is a fictitious interaction in which there is no energy loss, no change of direction, and no absorption. The second, with probability

$$\frac{\mu_{s1}}{\mu_2} ,$$

is a Compton scattering interaction. The third, with probability

$$\frac{\mu_{a1}}{\mu_2} ,$$

is a photoelectric absorption. The introduction of the fictitious interaction in medium 1 allows us to use the linear attenuation coefficient μ_2 for sampling path lengths in both medium 1 and medium 2. Thus, it is no longer necessary to compute the coordinates of the crossing point every time the photon crosses an interface or to check which of the various bounding surfaces has been crossed first.

In the present calculation, the above procedure was used in the source and capsule, and separately in the collimator. In the source

and capsule, cobalt was medium 2 and iron was medium 1. In the collimator, lead was medium 2 and iron was medium 1. (In principle, it would have been possible to base transport in the whole assembly on lead; however, this would have resulted in a very large number of fictitious interactions in the source and capsule, with attendant increase in computer time.)

The air column along the axis of the collimator was treated as a vacuum. Thus, when a photon entered this region, it was moved along its trajectory until it either re-entered the collimator wall or source capsule, or until it passed out the end of the collimator. For this reason, it was necessary to compute the coordinates of the crossing point when the photon crossed one of the surfaces bounding the air column.

The calculation of crossing point coordinates is very simple when the photon crosses a plane $z = z_b$. If the photon starts at the point (x_i, y_i, z_i) and moves along a path with direction cosines u_x, u_y , and u_z , then the distance s which the photon travels to reach the plane $z = z_b$ is ,

$$s = \frac{z_b - z_i}{u_z} .$$

The coordinates of the crossing point are given by,

$$x = x_i + su_x ,$$

$$y = y_i + su_y ,$$

$$z = z_b .$$

The calculation of crossing point coordinates is more complicated if the photon leaves the point (x_i, y_i, z_i) and crosses a cylindrical boundary with radius r . If x and y are the x - and y - coordinates of the crossing point, then

$$r^2 = x^2 + y^2 .$$

But x and y are given in terms of x_i and y_i by the equation,

$$x = x_i + su_x ,$$

$$y = y_i + su_y ,$$

where s is the distance from the point (x_i, y_i, z_i) to the crossing point. Therefore, s must satisfy the equation,

$$\begin{aligned}
 r^2 &= (x_1 + su_x)^2 + (y_1 - su_y)^2 \\
 &= x_1^2 + y_1^2 + 2s(u_x x_1 + u_y y_1) \\
 &\quad + s^2(u_x^2 + u_y^2) .
 \end{aligned}$$

Solving this equation, we find,

$$s = \frac{-(u_x x_1 + u_y y_1) \pm \sqrt{(u_x x_1 + u_y y_1)^2 + (u_x^2 + u_y^2)(r^2 - x_1^2 - y_1^2)}}{(u_x^2 + u_y^2)} .$$

The sign of the square root must be chosen according to the rules:

$$\begin{aligned}
 u_x x_1 + u_y y_1 &\geq 0, \quad r^2 > x_1^2 + y_1^2 \quad \text{plus sign;} \\
 u_x x_1 + u_y y_1 &< 0, \quad r^2 \geq x_1^2 + y_1^2 \quad \text{plus sign;} \\
 u_x x_1 + u_y y_1 &< 0, \quad r^2 < x_1^2 + y_1^2 \quad \text{minus sign.}
 \end{aligned}$$

Once s has been calculated, the coordinates of the crossing point are,

$$\begin{aligned}
 x &= x_1 + u_x s . \\
 y &= y_1 + u_y s , \\
 z &= z_1 + u_z s .
 \end{aligned}$$

Photon histories were terminated under the following conditions:

- (1) if a photon entered a black region; (2) if at a given interaction point a photoelectric interaction was selected. (3) if the photon energy dropped below 0.1 MeV in iron or cobalt, or below 0.2 MeV in lead; or (4) if the photon left the collimator.

When a photon emerged from the end of the collimator, either from the air column or from the surrounding iron and lead a score was recorded. The direction cosine u_z of the emergent photon was classified into one of the intervals $0.996 \leq u_z \leq 1.0$, $0.961 \leq u_z < 0.996$, or $0 \leq u_z < 0.961$ and its energy E was classified into one of 13, 0.1-MeV energy intervals between 0.1 and 1.4 MeV. The scoring procedure consisted of adding the statistical weight of the photon (always unity in the present calculation) to a running total for the appropriate energy angular interval.

The three angular groups defined above were of interest with respect to the University of Illinois 24-curie (nominal) experimental source. All uncollided photons which emerged without penetrating any part of the lip of the collimator had to have direction cosines $u_z > 0.996$, while photons which emerged with $u_z < 0.996$ had to penetrate some portion of the lip. For the experimental source, most of the photons which emerged with $u_z < 0.961$ had to penetrate an auxiliary lead collimator which was placed above the main collimator, as indicated in Figure 1.

III. RESULTS AND COMPARISON WITH OTHER WORK

The results of the calculation described in the preceding section are given in Table 1. The data are based on one million histories. This large number of histories was required because of the small angle of collimation and because of the fairly large number (39) of energy-angle groups used in the calculation. About 63 minutes on the IBM 7094 at the University of Illinois were required for the calculation.

An analytical calculation of the number of uncollided photons which one would expect to emerge from the collimator was made. Penetration of the lip of the collimator was neglected. Using the normalization of Table 1, the analytical calculation predicted 781 photons. From Table 1, we see that 948 photons emerge in the energy intervals 1.1 to 1.2 MeV and 1.3 to 1.4 MeV and the angular interval $0.966 \leq u_z \leq 1.0$. These photons may be regarded as uncollided. (An approximate estimate of the number of scattered photons contributing to the above-mentioned energy intervals appears to be between 10 and 20.) This means that approximately 17% of all uncollided photons emerging from the collimator have penetrated some portion of the lip.

The spectrum of gamma radiation emerging from the collimator in the angular interval $0.996 \leq u_z \leq 1.0$ is shown in Figure 2. Scattered photons contribute 16% of the area under the histogram. The low energy spectrum rises to a peak in the energy interval 0.2 to 0.3 MeV. The peak results primarily from the fact that the single-scattering cutoff energies for both source energies lie in this interval. The spectrum decreases rapidly below 0.2 MeV because of the increasing importance of the photoelectric effect at low photon energies.

TABLE 1

Number of photons per 0.1 MeV per 500,000 disintegrations of Co-60. The standard deviation for an entry in the table can be estimated by computing the square root.

Angular Interval Energy Interval (MeV)	$0.996 \leq u_z \leq 1.0$	$0.961 \leq u_z < 0.996$	$0 \leq u_z < 0.961$
$1.4 > E \geq 1.3$	493	7	0
$1.3 > E \geq 1.2$	3	18	1
$1.2 > E \geq 1.1$	455	31	8
$1.1 > E \geq 1.0$	13	36	26
$1.0 > E \geq 0.9$	6	17	19
$0.9 > E \geq 0.8$	11	8	25
$0.8 > E \geq 0.7$	14	4	19
$0.7 > E \geq 0.6$	12	9	14
$0.6 > E \geq 0.5$	19	8	14
$0.5 > E \geq 0.4$	22	3	14
$0.4 > E \geq 0.3$	30	1	11
$0.3 > E \geq 0.2$	36	5	4
$0.2 > E \geq 0.1$	16	5	3
Sum	1130	152	158

The spectrum in Figure 2 results almost entirely from scatterings in the source and capsule. This can be seen if we compare with one of the spectra computed by Preiss⁽¹⁾ for an uncollimated, encapsulated source. In Figure 3, Preiss's spectrum for his source B is compared with the spectrum in Figure 2. Preiss's source consisted of a cobalt metal disk inside a steel capsule. The cobalt disk had the same dimensions as the disk in Figure 1. The capsule had the same radial dimensions as the capsule in Figure 1, but its length was only 0.5 cm. Preiss's data were computed for $0.9 \leq u_z \leq 1.0$, but it seems reasonable to assume that the shape of the spectrum was practically constant over this range of directions, especially in view of the similarity of Preiss's results⁽¹⁾ for $0.9 \leq u_z \leq 1$ and $0 \leq u_z \leq 0.1$. The good agreement between our spectrum and Preiss's indicates that the spectrum in Figure 2 is affected predominantly by the top half-centimeter of the encapsulated source.

Costrell⁽²⁾ has measured spectra for a variety of encapsulated, Co-60 sources, both collimated and uncollimated. In Figure 4, the measured spectrum for his collimated source E2.5H is compared with the spectrum presented in Figure 2. His collimator was made of lead, was about 18 inches long, and had a diameter varying from $1 \frac{3}{16}$ inches at the source to $1 \frac{1}{2}$ inches at the mouth. The source consisted of a disk of cobalt metal with thickness 0.25 cm and diameter 1.7 cm. It was clad in aluminum of thickness 0.05 cm. The source was placed in a capsule made of steel and tungsten. The thickness of the source capsule between the cobalt and the end of the collimator was 0.035 inches of steel. The E2.5H source was selected for comparison because this thickness was almost the same as the corresponding thickness for the capsule in Figure 1. Agreement between the experimental and calculated results is quite good except in the energy interval 0.1 to 0.2 MeV.

Figures 5 and 6 show spectra for radiation which emerges in the angular intervals $0.961 \leq u_z < 0.996$ and $0 \leq u_z < 0.961$. Almost all the radiation emitted in these angular intervals must scatter at least once from the walls of the collimator. (Uncollided photons may contribute as much as 13% of the histogram area in Figure 5.) For every 100 photons which emerge from the collimator uncollided, i.e.

in the energy intervals 1.1 to 1.2 MeV and 1.3 to 1.4 MeV and in the angular interval $0.996 \leq u_z \leq 1.0$, about 16 photons are emitted in each of the direction intervals represented in Figures 5 and 6. It is interesting to note that most of these photons have energies greater than 0.5 MeV.

Cormack and Johns⁽⁵⁾ have reported a single-scattering calculation of the spectrum of radiation scattered from the walls of a collimator. Their collimator was made of lead and had a tapered opening with a minimum radius of 3 cm near the source and a maximum radius of 8 1/4 cm at a distance of 60 cm from the source. They calculated the spectrum at a point on the axis of the collimator 80 cm from the source.

In Figure 7, we have summed the spectra presented in Figures 5 and 6 and normalized to one uncollided photon emerging from the collimator. The shaded portion of the histogram represents the contribution from the direction interval $0.961 \leq u_z < 0.996$. The curve is the spectrum calculated by Cormack and Johns. It rises to a maximum value of about 2.5 at an energy of 1.13 MeV and then cuts off sharply. In the Monte Carlo calculation, the sharp peak is smeared out over several energy intervals, largely because of use of a finite sized source and detector.

Because of considerable geometric differences, we expect at best only qualitative agreement between the results of Cormack and Johns and the results in this report. Consequently, the near equality between the area under the curve and the area of the shaded histogram is probably somewhat fortuitous. The largest angle which radiation directions could have with respect to the axis of the collimator and be included in the calculation of Cormack and Johns was about 22° . The largest angle which was included in the calculation of the shaded histogram was about 16° ($\approx \cos^{-1} 0.961$). Considering only these two angles, we might therefore expect the area under the curve to be greater than the area of the shaded histogram. On the other hand, the lead collimator scatters radiation less efficiently than the steel liner of the collimator in Figure 1. It thus appears that the larger angle of acceptance in the Cormack and Johns calculation is approximately compensated by the relatively poorer scattering characteristics of lead.

IV. CONCLUSION

The data presented in this report show that roughly 17% of the photons which emerge with their initial energies from the collimator in Figure 1 have penetrated some portion of the lip of the collimator. This number could probably be reduced somewhat if the steel liner of the collimator were replaced by lead.

It was also observed that for every 100 photons which are emitted from the collimator without energy loss, approximately 32 photons are scattered by the collimator wall and emerge along directions which cannot "see" the source directly. Most of these photons have energies in excess of 0.5 MeV with the most probable energy being about 1 MeV. This result is in qualitative agreement with earlier calculations published by Cormack and Johns⁽⁵⁾. These collimator-scattered photons were not observed in the experimental measurements of Costrell⁽²⁾ mainly because of the geometrical arrangement in which his measurements were made.

REFERENCES

1. Preiss, K., "Monte Carlo Calculation of Self Shielding by Encapsulated Gamma Ray Sources," University of Illinois, NRSS No. 3, August 1966.
2. Costrell, L., "Scattered Radiation from Large Co-60 Calibrating Sources," Health Physics, Vol. 8, p. 261, 1962.
3. Scrimger, J. W. and Cormack, D. V., "Spectrum of the Radiation from a Co-60 Teletherapy Unit," Brit. J. Radiology, Vol. 36, No. 427, p. 514, 1963.
4. Aitken, J. H. and Henry, W. H., "Spectra of the Internally Scattered Radiation from Large Co-60 Sources Used in Teletherapy," International J. of App. Radiation and Isotopes, Vol. 15, p. 713, 1964.
5. Cormack, D. V. and Johns, H. E., "Spectral Distribution of Scattered Radiation from a Kilocurie Cobalt-60 Unit," Brit. J. Radiology, Vol. 31, No. 369, p. 497, 1958.
6. Woodcock, E. R., Murphy, T., Hemmings, P. J., Longworth, T. C., "Techniques Used in the Gem Code for Monte Carlo Neutronics Calculations in Reactors and Other Systems of Complex Geometry," Argonne National Laboratory, Report 7050, USEAC Report TID 4500, May 1965.
7. Hubbell, J. H. and Berger, M. J., "Photon Attenuation and Energy Absorption Coefficients, Tabulations and Discussion," to be published in Engineering Compendium on Radiation Shielding, Springer-Verlag, Berlin and New York.
8. Kahn, H., "Applications of Monte Carlo," USEAC Report R-1237, April 1954.

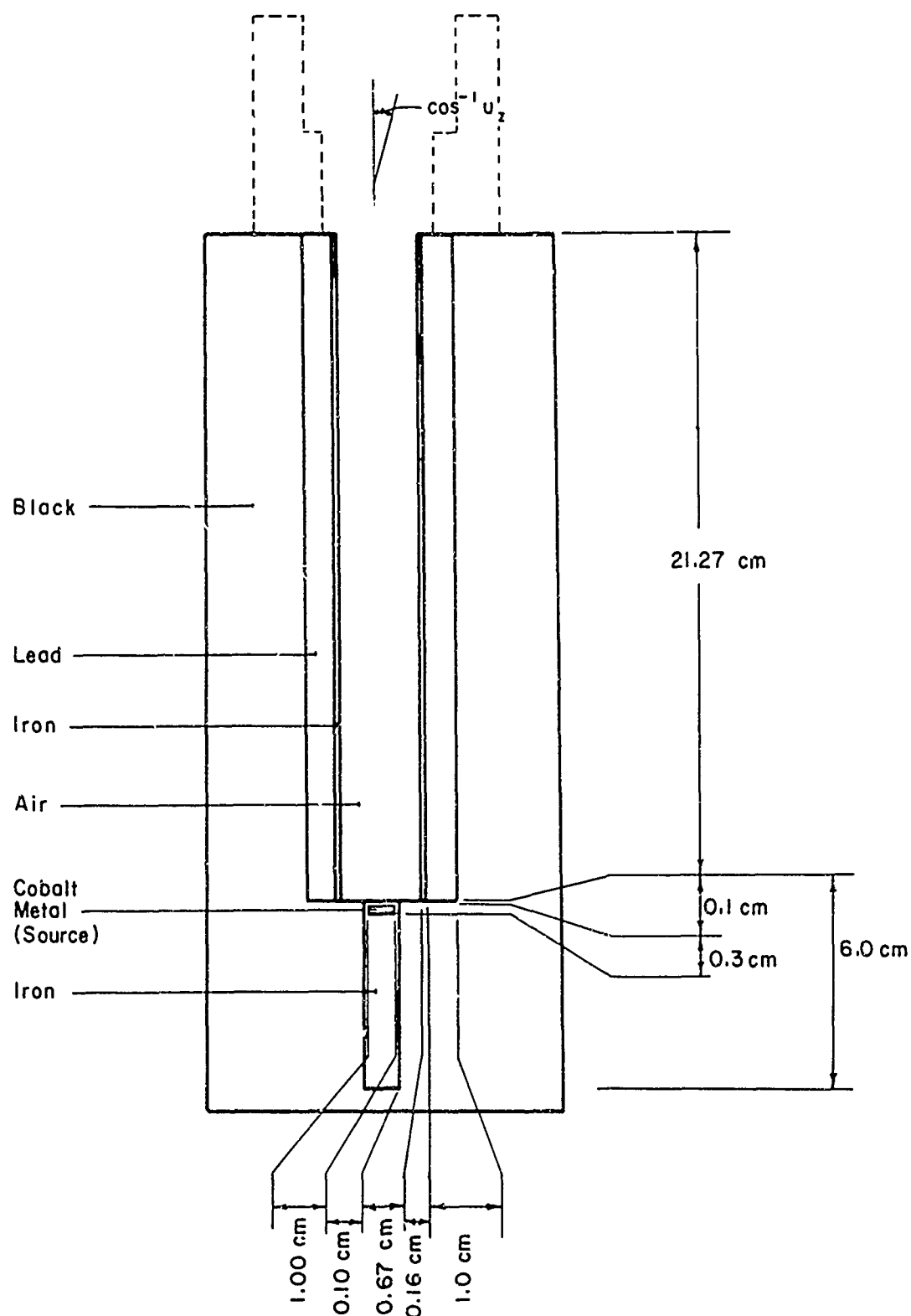


Figure 1. Source in collimator. The position of an auxiliary collimator which was placed on the main collimator when the experimental source was in use is indicated by the dashed lines at the top of the figure. The auxiliary collimator was not included in the computational model.

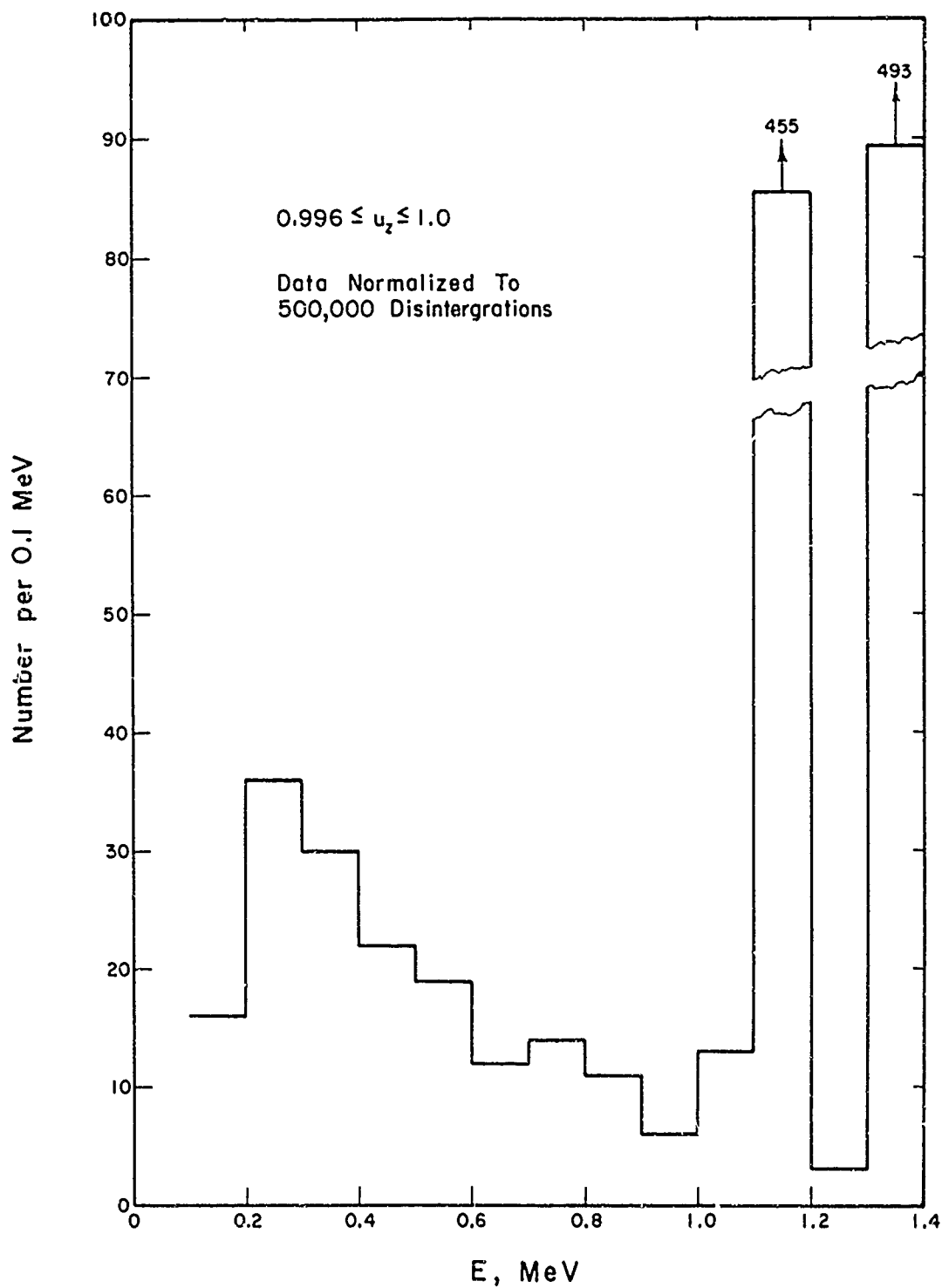


Figure 2. Spectrum of radiation emerging from the collimator in the direction interval $0.996 \leq u_z \leq 1.0$. Photons in the energy intervals 1.1 to 1.2 MeV and 1.3 to 1.4 MeV are regarded as uncollided. If normalization to 1 curie is desired, multiply the given ordinates by 7.4×10^4 .

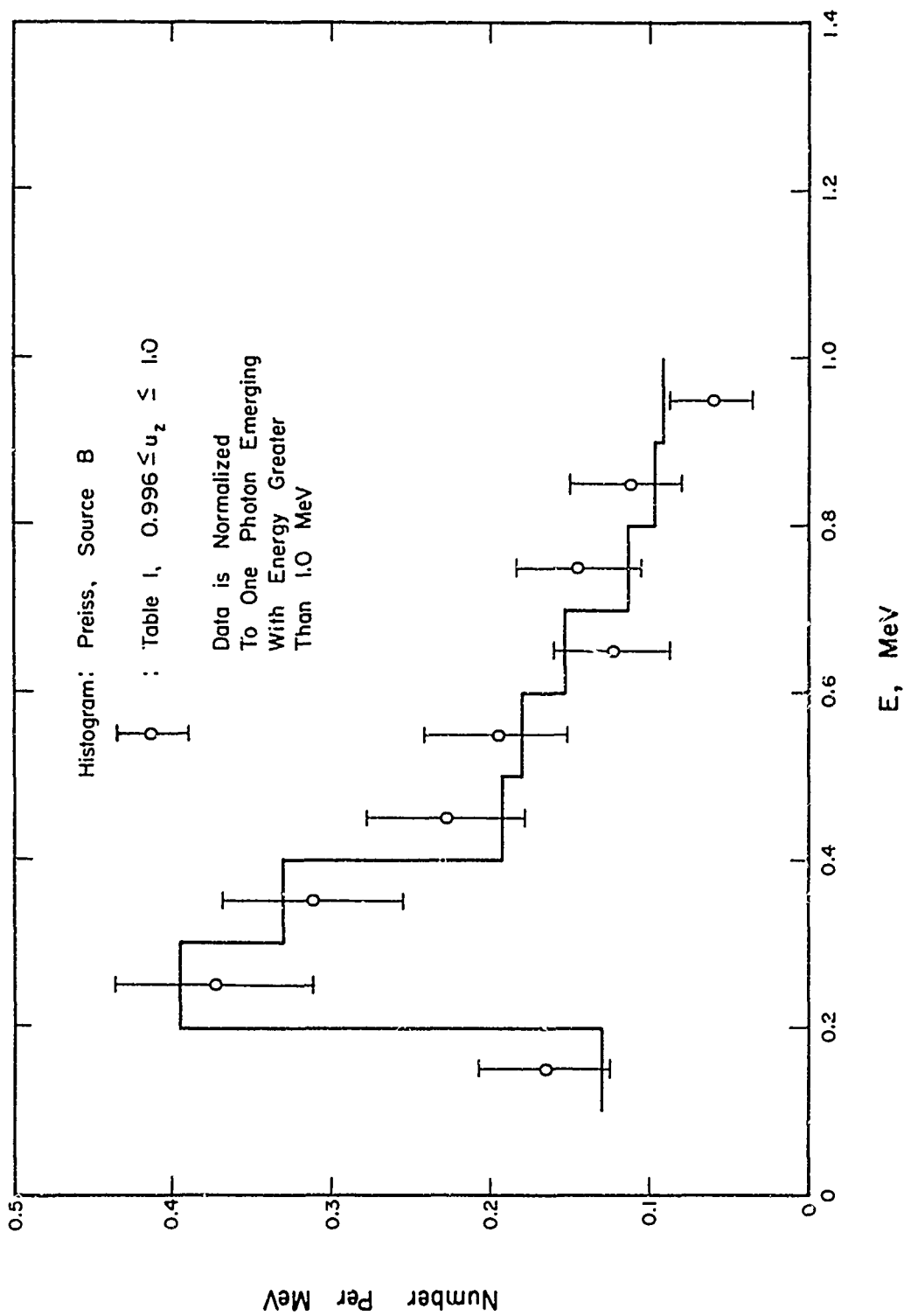


Figure 3. Comparison with spectrum calculated by Preiss for an uncollimated source. Error bars indicate standard deviation of our Monte Carlo results.

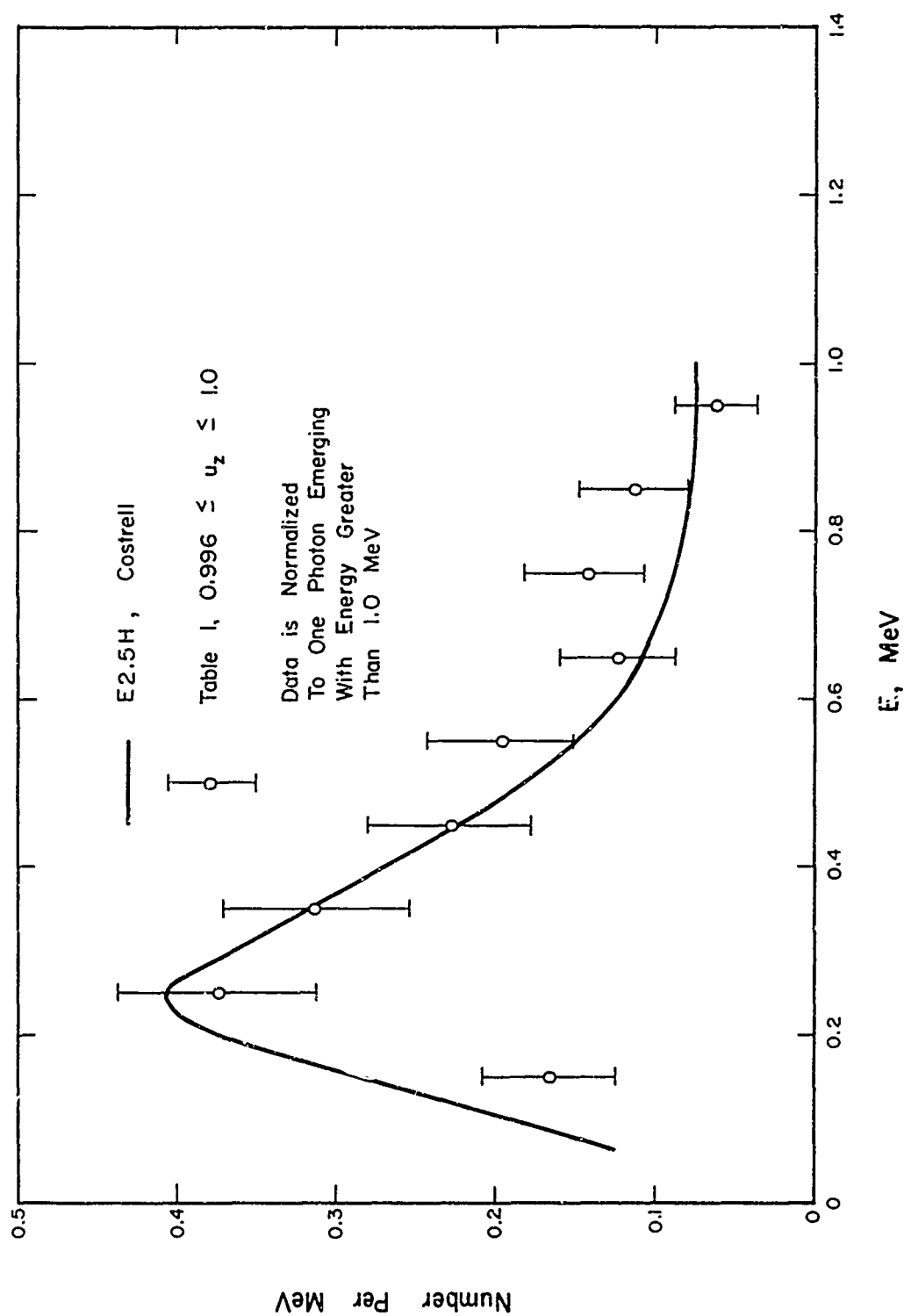


Figure 4. Comparison with spectrum measured by Costrell for a collimated source. Error bars indicate standard deviation of our Monte Carlo results.

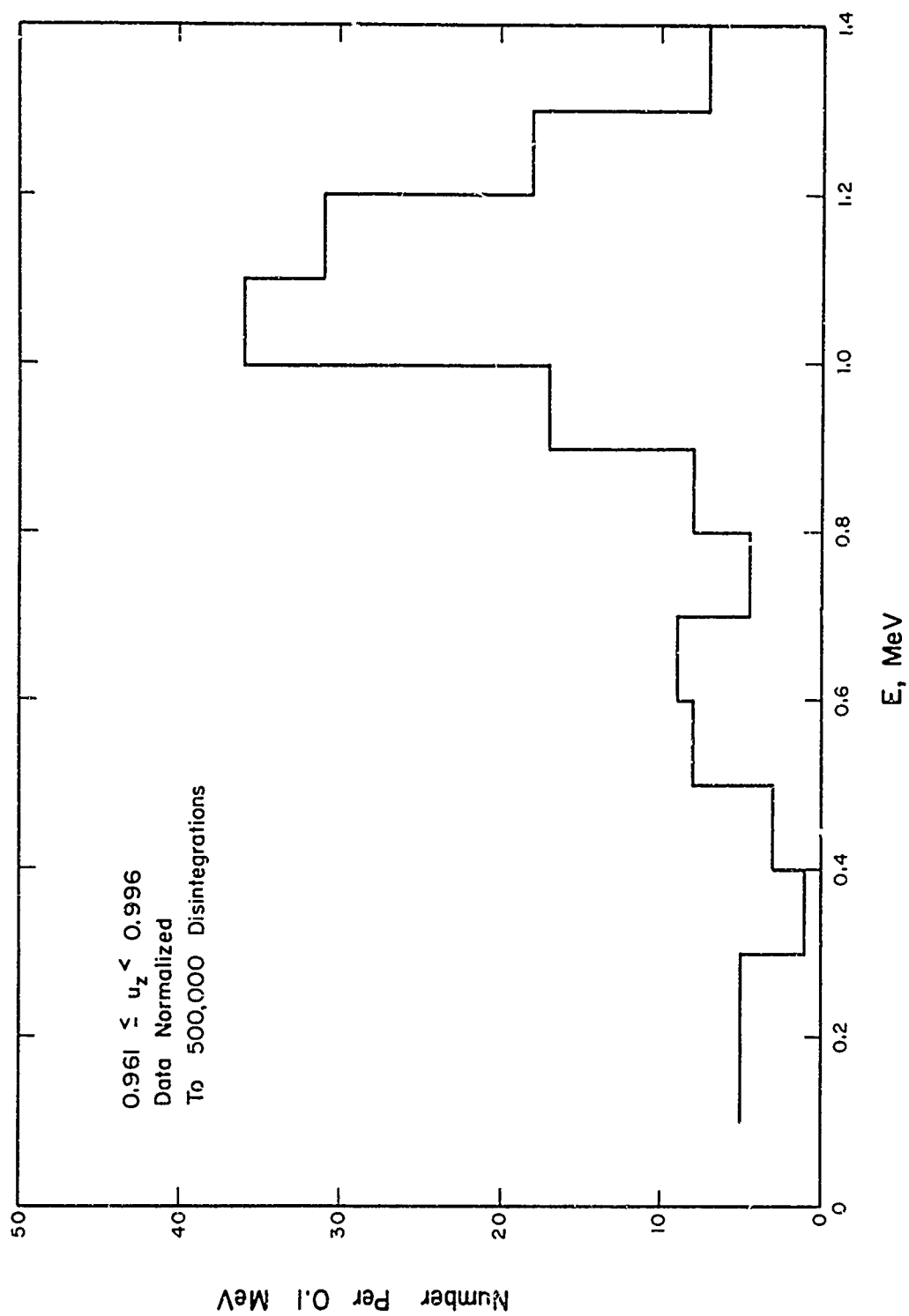


Figure 5. Spectrum of radiation emerging from the collimator in the direction interval $0.961 \leq u_z < 0.996$.

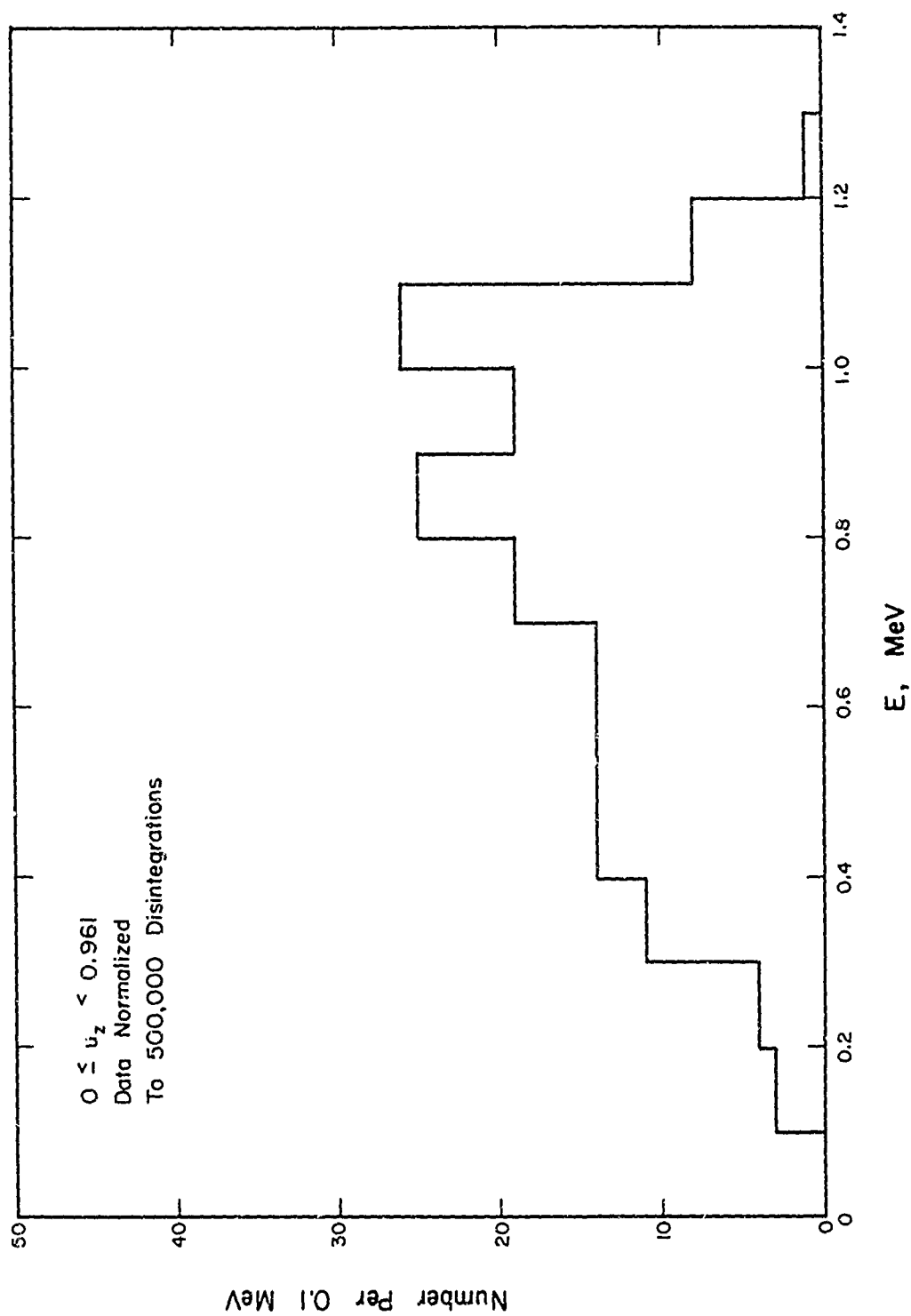


Figure 6. Spectrum of radiation emerging from the collimator in the direction interval $0 \leq u_z < 0.961$.

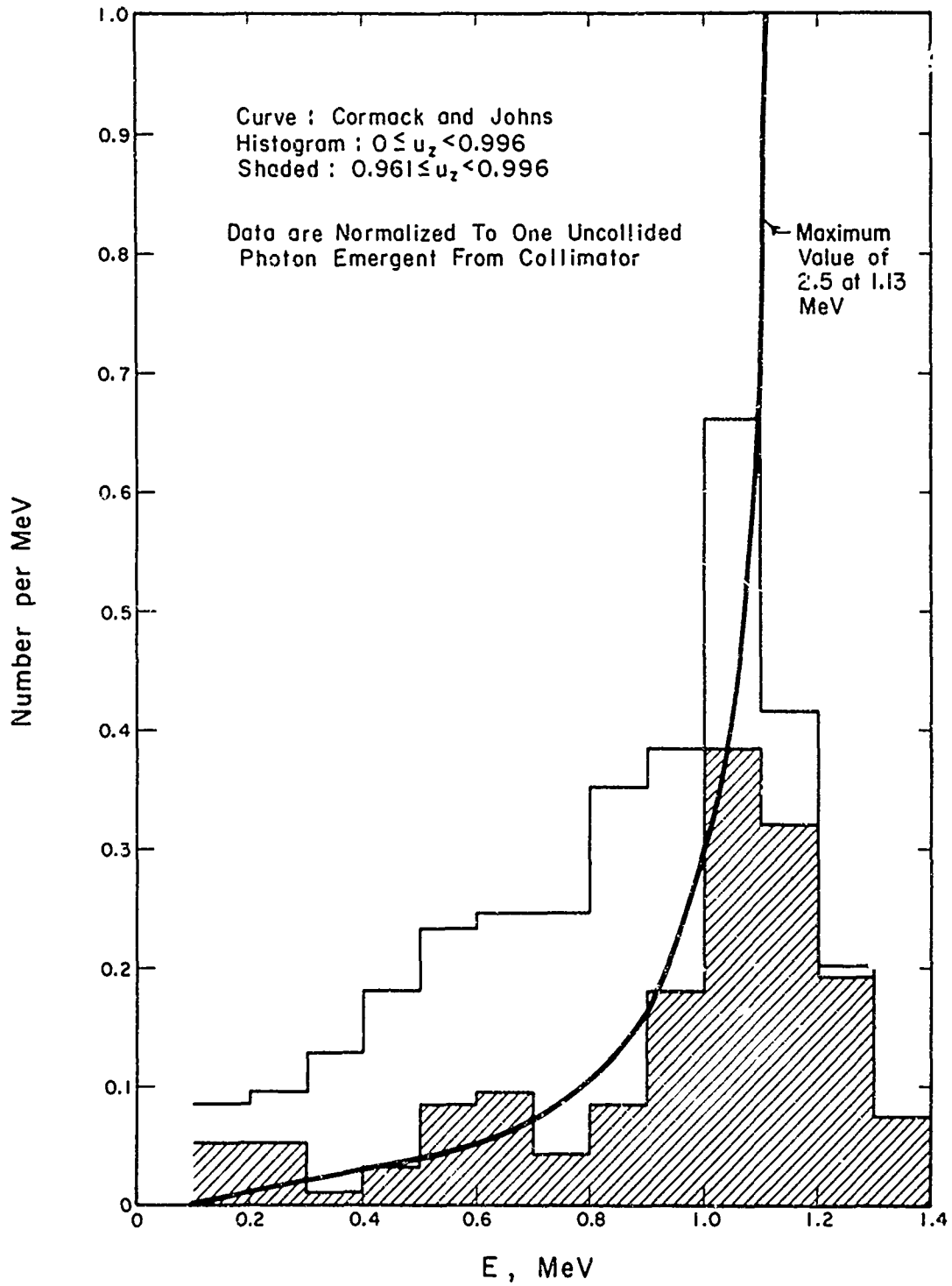


Figure 7. Comparison of present results with calculation by Cormack and Johns of the spectrum of radiation singly scattered from the walls of a collimator.

APPENDIX AFILTERED SPECTRA

For use in experimental work at the University of Illinois, it was necessary to modify the collimator emergent spectrum of Figure 2 by assuming that radiation from the collimator subsequently passed perpendicularly through a thin lead sheet. A simple filtered spectrum was calculated in which scattering by the lead sheet was neglected. The results are given in Table A1. In the column for zero thickness, the spectrum was normalized to one photon with energy greater than 0.1 MeV. In the other columns, for a given energy interval, the number to the left of the slash was obtained by multiplying the corresponding number from the unfiltered spectrum by an exponential factor. The attenuation coefficient was evaluated at the mid-point energy of the interval. The number to the right of the slash resulted from renormalizing the filtered spectrum to one photon with energy greater than 0.1 MeV.

The spectra in Figures 2 and 5 were added together and filtered as described above for the spectrum in Figure 2. The resulting spectra for this case are presented in Table A2.

TABLE A1

Number of photons per 0.1 MeV for $0.996 \leq u \leq 1.0$
which are transmitted by lead sheets of different
thicknesses.

Filter Thickness (inches) Energy Interval (MeV)	0	1/8	1/4
1.4 > E ≥ 1.3	0.436	0.358/0.474	0.294/0.491
1.3 > E ≥ 1.2	0.003	0.002/0.003	0.002/0.003
1.2 > E ≥ 1.1	0.403	0.324/0.429	0.261/0.435
1.1 > E ≥ 1.0	0.011	0.009/0.012	0.007/0.012
1.0 > E ≥ 0.9	0.005	0.004/0.005	0.003/0.005
0.9 > E ≥ 0.8	0.010	0.007/0.010	0.005/0.009
0.8 > E ≥ 0.7	0.012	0.009/0.012	0.006/0.011
0.7 > E ≥ 0.6	0.011	0.007/0.010	0.005/0.008
0.6 > E ≥ 0.5	0.017	0.010/0.014	0.006/0.011
0.5 > E ≥ 0.4	0.020	0.010/0.013	0.005/0.009
0.4 > E ≥ 0.3	0.026	0.010/0.013	0.003/0.006
0.3 > E ≥ 0.2	0.032	0.004/0.005	0.001/0.001
0.2 > E ≥ 0.1	0.014	0	0

TABLE A2

Number of photons per 0.1 MeV for $0.961 \leq u_z < 1.0$
which are transmitted by lead sheets of different
thicknesses.

Filter Thickness (inches) Energy Interval (MeV)	0	1/8	1/4
$1.4 > E \geq 1.3$	0.390	0.320/0.426	0.263/0.443
$1.3 > E \geq 1.2$	0.016	0.013/0.018	0.011/0.018
$1.2 > E \geq 1.1$	0.379	0.305/0.406	0.245/0.413
$1.1 > E \geq 1.0$	0.038	0.030/0.040	0.024/0.040
$1.0 > E \geq 0.9$	0.018	0.014/0.018	0.011/0.018
$0.9 > E \geq 0.8$	0.015	0.011/0.015	0.008/0.014
$0.8 > E \geq 0.7$	0.014	0.010/0.013	0.007/0.012
$0.7 > E \geq 0.6$	0.016	0.011/0.015	0.008/0.013
$0.6 > E \geq 0.5$	0.021	0.013/0.017	0.008/0.014
$0.5 > E \geq 0.4$	0.020	0.010/0.014	0.005/0.009
$0.4 > E \geq 0.3$	0.024	0.009/0.012	0.003/0.005
$0.3 > E \geq 0.2$	0.032	0.004/0.005	0.001/0.001
$0.2 > E \geq 0.1$	0.016	0	0
Total	1.00	0.750/1.00	0.594/1.00

APPENDIX BMASS ATTENUATION COEFFICIENTS

The mass attenuation coefficient data used in the calculation are listed in Table B1. The coefficients for iron and lead are from tabulations of Hubbell and Berger.⁽⁷⁾ Since Hubbell and Berger did not include data for cobalt in their tabulations, data for this element were generated by a separate calculation as follows:

The total Compton interaction cross section was calculated using a tabulation of the Klein-Nishina formula. The cross sections for three other processes, viz., photoelectric effect, pair production in the field of the nucleus, and pair production in the field of an electron, were determined by an interpolation procedure using microscopic cross section data for iron and copper. Three primary steps were involved in the interpolation.

1. A dominant functional dependence on the atomic number Z was removed from the cross section data for iron and copper by division.
2. For fixed energy, a linear interpolation was performed on the data for iron and copper to get corresponding data for cobalt.
3. The cobalt data resulting from Step 2 were multiplied by the function of Z removed in Step 1.

The functional dependences assumed were $Z^{4.5}$ for the photoelectric effect, Z^2 for pair production in the field of the nucleus, and Z for pair production in the field of an electron.

TABLE B1

Mass Attenuation Coefficients (cm^2/g)*

Energy (MeV)	Iron	Cobalt	Lead
0.010	172.0	187.0	132.0
0.015	55.7	60.8	112.0
0.020	25.1	27.4	83.4
0.030	7.87	8.67	27.9
0.040	3.46	3.82	13.0
0.050	1.84	2.02	7.17
0.060	1.13	1.24	4.47
0.080	0.550	0.596	2.12
0.100	0.342	0.365	5.62
0.150	0.184	0.189	1.99
0.200	0.139	0.140	0.969
0.300	0.107	0.106	0.385
0.400	0.0921	0.0911	0.221
0.500	0.0829	0.0818	0.154
0.600	0.0761	0.0751	0.120
0.800	0.0664	0.0655	0.0856
1.000	0.0596	0.0587	0.0689
1.500	0.0486	0.0479	0.0509
2.000	0.0425	0.0419	0.0450
3.000	0.0361	0.0357	0.0415
4.000	0.0331	0.0328	0.0415
5.000	0.0315	0.0313	0.0424
6.000	0.0305	0.0304	0.0434
8.000	0.0299	0.0299	0.0460
10.000	0.0299	0.0300	0.0487

* The densities assumed were 7.86 g/cm^3 for iron, 8.71 g/cm^3 for cobalt, and 11.43 g/cm^3 for lead. The density for lead should have been 11.34 g/cm^3 . The influence of this mistake on the final results is expected to be negligible.

APPENDIX CDESCRIPTION OF FORTRAN PROGRAM CØLLIMATØRC.1 General Remarks

CØLLIMATØR performs a Monte Carlo calculation of gamma ray transport in a finite, multi-region medium having cylindrical symmetry. Boundaries of regions are defined by the walls of concentric cylinders and by planes passing through these cylinders perpendicular to their axis. A particular region is identified by a radial index NR and a vertical index NZ. A radial index NR indicates that the region is between concentric cylinders numbered NR and NR + 1. The innermost cylinder is assigned the number two. Similarly, a vertical index NZ means that the region lies between planes numbered NZ and NZ + 1.

In addition, each region is assigned three other indexes: MAT, MAT2, and NSPL. MAT is called pseudo-material index. If it is positive, it identifies the material whose attenuation coefficient is to be used for sampling path lengths in the region (see Section II). If it is zero, the region is void. The value -1 indicates that the region is black and the value -2 labels the region as a detector.

The index MAT2 is either positive or zero. It identifies the actual material in the region. If for a particular region its value is different from the value of MAT for the region, the fictitious interaction described in Section II is introduced as an alternative to photoelectric absorption or Compton scattering. MAT2 is assigned the value zero for detector regions, black regions, and voids.

The third index, NSPL, is a splitting parameter. Splitting was not used in the calculation for this report, but the program was written to allow for this possibility. If the NSPL value for a region is zero, then no splitting occurs in that region. If the value of NSPL is greater than zero, then upon interacting in the region, a photon is split into NSPL new photons. The statistical weight assigned to these new photons is the statistical weight of the original photon divided by NSPL. When a splitting occurs, the radial and vertical index of the region, the coordinates of the interaction point, the statistical weight, the photon

energy, and the direction cosines of the photon are stored. The history for each newly generated photon is then followed in turn until the histories of all the photons have been completed. A photon which results from a splitting may itself be split if it has a subsequent interaction in a region where NSPL is different from zero. A logic diagram for a CØLLIMATØR history with splitting included is shown in Figure C1. In the diagram, ISPL is an index which counts the number of interaction points where splitting has occurred.

C.2 Description of Individual Subroutines

CØLLIMATØR (Main Program)

Subroutine called: LEARN, DATEX, TRACK, TEACH.

The program consists of a nest of five loops. The index NZSØ specifies the z coordinate of the source point, NRSØ the x coordinate of the source point, (the y coordinate of the source point is always zero), NESØ specifies the source energy, and NSPE counts the number of histories completed for each source point, source energy combination. The product $NSEG \times NESX \times NPSX \times NZSX \times LP$ is the total number of histories to be done.

Subroutine LEARN

Subroutine called: none.

All input data are read by this program. After the data have been read, they are immediately printed under headings which give either the variable name or a brief description of the variable.

The first card read contains 72 alphanumeric characters and when printed at the beginning of the calculation serves to identify the run. Input variables are listed and defined below in the order in which they occur in the subroutine.

NRAN: The number of random numbers to be rejected before starting the calculation.

NEAX: The number of energy intervals to be used in the calculation of spectra.

NTHX: The number of angular intervals to be used in calculating the directional distribution.

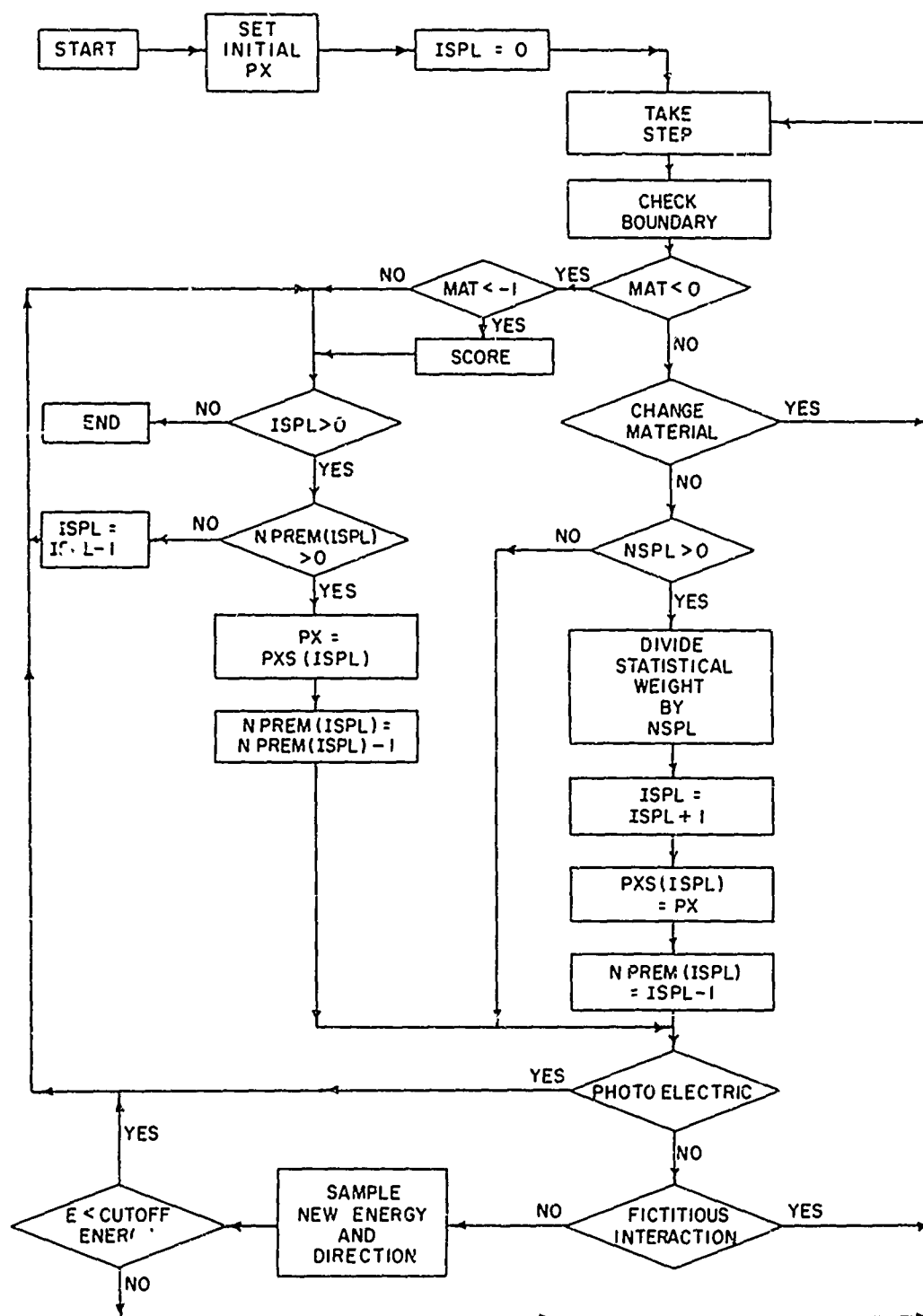


Figure C1. Flow diagram of a COLLIMATOR history. PX stands for photon energy, direction, statistical weight, vertical index, and radial index.

MXAX: The number of energies for which tabulated cross section data are to be read.
 MATX: The number of materials in the collimator. In the present calculation, there were three; iron, cobalt, and lead.
 NRAX: The number of radial boundaries.
 NZAX: The number of horizontal boundaries.
 NZTP: The index of the horizontal plane bounding the top of the collimator.
 NRWL: The index of the radial boundary of the air column.
 NZBT: The index of the horizontal plane bounding the bottom of the air column.
 IHIX: This integer must be divisible by the product $NESX * NRSX * NZSX$.
 LP: The product of LP and IHIX determines the number of histories to be done.
 NESX: The number of source energies. Each source energy is regarded as equally likely.
 NRSX: The number of x-coordinates for source points.
 NZSX: The number of z-coordinates for source points. The number of source points is $NZSX * NRSX$.
 NR1: The radial index of the source region.
 NZ1: The vertical index of the source region.
 NASX: This index will be discussed later with the variable CTHØ and SØANG.
 MAT,
 MAT2: These variables were discussed in the general remarks at the beginning of this Appendix.
 ESØ: A list of source energies.
 ZH: A list of horizontal boundaries.
 RHØ: A list of cylindrical boundaries. The first number in this list should be zero.
 DEN: A list of densities for the materials in the collimator.
 EB: A list of energies for which cross section data are to be read. This list is read for each material but must be the same for each material.
 XSECB: This is a list of interaction coefficients. If the indices specified for this variable are (M,1,NMAT), then we have the Compton interaction coefficient for the M'th energy, and the material

with index NMAT. If the index 1 is replaced by 2, then we have the total attenuation coefficient. Note that if the densities were read in the order iron, cobalt, and lead, then the interaction coefficients must be read in the same order.

DUM1,
DUM2,
DUM3,

DUM4: These are variables which are used to skip interaction coefficient data on the input cards which are not used in the calculation.

CTH: A list of lower limits for the intervals in which μ_z is classified for the directional distribution.

ECLS: A list of lower limits for the energy intervals used in the calculation of spectra.

NSPL: The splitting parameters were discussed in the general remarks at the beginning of this appendix. They should not be given the value one since this accomplishes the same thing as the value zero but increases the amount of bookkeeping required.

CTH0,
S0ANG,

NASX: The program assumes that each source point emits radiation isotropically. However, it may be desirable to sample more photons in a certain range of directions and give them smaller weight while sampling fewer in other directions and giving them larger weight. These variables define a cumulative probability distribution at NASX values of the direction cosine relative to the z-axis. The probability distribution is assumed to be in histogram form. To sample all directions with equal probability, we read in the following table:

CTH0	S0ANG
-1	0.0
1	1.0

The values of S0ANG must be in increasing order.

IWCT: For each material in the collimator, this variable lists the index of one of the energies in the list ECLS. We are thus able to specify different cutoff energies in different materials in the collimator.

Subroutine DATEX

Subroutines called: RAM2B, TABIN.

The tasks of this subroutine are listed below in the order in which they are done.

1. Rejects NRAN random numbers.
2. Re-arranges the tables of interaction coefficients so that the list EB is in descending order and multiplies the interaction coefficients for each material by the density. Since log-log interpolation is used, it takes logarithms of EB and XSECB.
3. Prepares an expanded table of interaction coefficients for 300 energies between zero and 1.5 MeV. The energy interval 0.005 MeV is used over the entire range. Hereafter, when an interaction coefficient is desired for an energy E, rather than interpolate, we compute an index using the formula $NE = 200.0 * E + 0.5$ and use the entry in these expanded tables corresponding to this index.
4. A table of sines and cosines is generated for 360 angles starting at 0.5° and proceeding in steps of 1° up to and including 359.5° . The sine and cosine for a random angle between 0° and 360° are then selected by computing an index according to the formula $IPH = 360.0 * RAN$, where RAN is a random number, and then choosing the sine and cosine in this table corresponding to the index $IPH + 1$.
5. A list RHØ2 of the squares of the radii of the cylindrical boundaries is generated.
6. Lists of source point coordinates RSØ and ZSØ are generated.
7. A list PART of floating point values of NSPL is generated.
8. Variables in which scores are accumulated, SPEC and SPEC2, are initially set equal to zero.
9. The cutoff energy for each material is expressed in terms of its Compton wavelength.

Subroutine TRACK

Subroutines called: RAM2B, CHECK, VACUØ, COMPT2, GRADE.

This subroutine performs the following tasks:

1. Source position, energy, and direction are selected to start a photon history. The energy of the photon is expressed in terms of the Compton wavelength.
2. Distances between interaction points are sampled.
3. The type of interaction is selected.
4. If splitting is used, the necessary bookkeeping is performed by this subroutine.

Subroutine CHECK

Subroutines called: none.

Without going into very much detail, we may outline the operation of the subroutine by the following steps:

1. It checks to see if a horizontal boundary has been crossed. If it has, it then checks to see if a cylindrical boundary was crossed first.
2. If a horizontal boundary has not been crossed, it checks to see if a cylindrical boundary has been crossed. If not, it sets the index NSCT = 1 and returns to TRACK.
3. If a boundary is crossed, it compares the index MAT for the new region with MAT for the region where the photon started. If MAT is the same for both regions, then NR and NZ, the radial and vertical indices (see the general remarks at the beginning of this Appendix) are set equal to values appropriate to the new region. It then checks as in steps one and two to see if the photon actually stops in the new region or crosses into still another region. When a photon has stopped in a region, the subroutine sets NSCT = 1 and returns to TRACK.
4. If MAT for the region where the photon started and MAT for the new region are different, the coordinates of the crossing point are computed. It sets NSCT = 0 and returns to TRACK.
5. If MAT for the new region is negative, the subroutine does not compute crossing point coordinates but immediately returns to TRACK.

Subroutine VACUØ

Subroutines called: none.

Control is transferred to this subroutine when the photon enters the air column. The coordinates of the point where the photon crossed into the air are given. The subroutine moves the photon along its current trajectory until the photon leaves the collimator or re-enters some part of the collimator. If the photon re-enters the collimator or source capsule, the coordinates of the re-entry point are computed.

Subroutine COMPT2

Subroutine called: RAM2B.

This subroutine uses the method of Kahn⁽⁸⁾ to sample a new photon direction and energy from the Klein-Nishina distribution.

Subroutine GRADE

Subroutines called: none.

When a photon enters a region designated as a detector, the subroutine adds the statistical weight of the photon to SPEC for the appropriate energy, angular interval. The squares of individual scores are cumulated in SPEC2.

Subroutine TEACH

Subroutine called: none.

This subroutine normalizes and prints the data. It also computes the fractional standard deviation of all results. In addition, the spectrum which is obtained by summing over all direction intervals and the directional distribution summed over all energy intervals are printed.

Liberal use is made of printed headings over all output data. This makes the output fairly self-explanatory.

Subroutine TABIN

Subroutines called: none.

This subroutine performs a three-point interpolation simultaneously on each of MMAX functions of a single independent variable. XB is the list of independent variable values for which the functional values FB are given, and must be stored in descending order. NMAX is the number of values XB in the list and must be ≥ 3 . FX contains the list of functional values interpolated at X.

The index NTABIN must be unity the first time the subroutine is called. The subroutine then computes and stores certain differences and products which will be used over and over. Once this has been done, NTABIN is set equal to two so that these differences need not be computed again on subsequent calls.

Functional Subroutine RAM2B

This function is used to generate a sequence of random numbers uniformly distributed between zero and one. It is written in machine language. The multiplicative congruential method is used. The multiplier is 5^{15} and the modulus is 2^{35} . The first number in the sequence is always $[5^{15}(2^{35} - 1)] \pmod{2^{35}}$. Thus, to change the initial random number, one rejects several random numbers before beginning the calculation.

C.3 Program Listings and Sample Output

Listings of the various FORTRAN programs are given on the following pages. The computer output for the calculation described in this report is reproduced following the listings.

```

$      FASTRAN
C      COLLIMATOR                                4-20-67
C      CALCULATES THE ENERGY-ANGLE SPECTRUM OF RADIATION EMERGING
C      FROM A COLLIMATED SOURCE OF GAMMA RADIATION
      DIMENSION CPH(360),CTH(20),DEN(4),EB(25),ECLS(30),MAT(10,10),
1     MAT2(10,10),NEREM(50),NPREM(50),NRREM(50),NSPL(10,10),
2     NZREM(50),PART(10,10),RHO(10),RHO2(10),RSO(10),SPEC(20,30),
3     SPEC2(20,30),SPH(360),UC(300,4),UT(300,4),UXREM(50),
4     UYREM(50),UZREM(50),WREM(50),WTREM(50),XREM(50),XSEC(2,4),
5     XSECB(25,2,4),YREM(50),ZH(10),ZREM(50),ZSO(10)
      DIMENSION ESO(2),CTHO(10),SOANG(10),IWCT(4),WMAX(4)
      COMMON CPH,CTH,DEN,EB,ECLS,ESO,IHIX,MAT,MAT2,MATX,MXAX,
1     NE,NEAX,NEREM,NESO,NESX,NPREM,NR,NR1,NRAN,NRAX,NRREM,NRSO,
2     NRSX,NRWL,NSCT,NSEG,NSPL,NTHX,NZ,NZ1,NZAX,NZBT,NZREM,NZSO,
3     NZSX,NZTP,PART,RAN,RHO,RHO2,RSO,S,SPEC,SPEC2,SPH,SUZ,UC,UT,
4     UX,UXREM,UY,UYREM,UZ,UZREM,W,WMAX,WREM,WT,WTREM,X,XN,XREM,
5     XSEC,XSECB,Y,YN,YREM,Z,ZH,ZN,ZREM,ZSO
      COMMON CTHO,IWCT,NASX,SOANG,LP
      CALL LEARN
      CALL DTEX
      L=0
5     L=L+1
      NZSO=0
10    NZSO=NZSO+1
      NRSO=0
20    NRSO=NRSO+1
      NESO=0
30    NESO=NESO+1
      NSPE=0
40    NSPE=NSPE+1
      CALL TRACK
      IF(NSPE-NSEG)40,50,50
50    IF(NESO-NESX)30,60,60
60    IF(NRSO-NRSX)20,70,70
70    IF(NZSO-NZSX)10,80,80
80    IF(L-LP)5,90,90
90    CALL TEACH
      CALL SYSTEM
      END

```

```

$      FASTRAN
C      SUBROUTINE LEARN                                4-20-67
C      READS ALL INPUT DATA
      SUBROUTINE LEARN
      DIMENSION CPH(360),CTH(20),DEN(4),EB(25),ECLS(30),MAT(10,10),
1     MAT2(10,10),NEREM(50),NPREM(50),NRREM(50),NSPL(10,10),
2     NZREM(50),PART(10,10),RHO(10),RHO2(10),RSO(10),SPEC(20,30),
3     SPEC2(20,30),SPH(360),UC(300,4),UT(300,4),UXREM(50),
4     UYREM(50),UZREM(50),WREM(50),WTREM(50),XREM(50),XSEC(2,4),
5     XSECB(25,2,4),YREM(50),ZH(10),ZREM(50),ZSO(10)
      DIMENSION ESO(2),CTHO(10),SOANG(10),IWCT(4),WMAX(4)
      COMMON CPH,CTH,DEN,EB,ECLS,ESO,IHIX,MAT,MAT2,MATX,MXAX,
1     NE,NEAX,NEREM,NESO,NESX,NPREM,NR,NR1,NRAN,NRAX,NRREM,NRSO,
2     NRSX,NRWL,NSCT,NSEG,NSPL,NTHX,NZ,NZ1,NZAX,NZBT,NZREM,NZSO,
3     NZSX,NZTP,PART,RAN,RHO,RHO2,RSO,S,SPEC,SPEC2,SPH,SUZ,UC,UT,

```

```

4  UX,UXREM,UY,UYREM,UZ,UZREM,W,WMAX,WREM,WT,WTREM,X,XN,XREM,
5  XSEC,XSECB,Y,YN,YREM,Z,ZH,ZN,ZREM,ZSO
COMMON CTHO,IWCT,NASX,SOANG,LP
WOT6,10
10 FORMAT(1H0)
RIT7,20
WOT6,20
20 FORMAT(72H
1
WOT6,10
WOT6,30
30 FORMAT(72H NRAN NEAX NTHX MXAX MATX NRAX NZAX NZTP NRWL
1NZBT IHIX LP)
RIT7,45,NRAN,NEAX,NTHX,MXAX,MATX,NRAX,NZAX,NZTP,NRWL,NZBT,IHIX,LP
WOT6,45,NRAN,NEAX,NTHX,MXAX,MATX,NRAX,NZAX,NZTP,NRWL,NZBT,IHIX,LP
40 FORMAT(12I6)
45 FORMAT(10I6,18,14)
WOT6,10
WOT6,50
50 FORMAT(36H NESX NRSX NZSX NR1 NZ1 NASX)
RIT7,40,NESX,NRSX,NZSX,NR1,NZ1,NASX
WOT6,40,NESX,NRSX,NZSX,NR1,NZ1,NASX
WOT6,10
WOT6,60
60 FORMAT(65H INDICES TO IDENTIFY PSEUDO-MATERIAL IN EACH REGION OF C
1OLLIMATOR)
DO 70 NZ=1,NZAX
RIT7,40,(MAT(NR,NZ),NR=1,NRAX)
WOT6,40,(MAT(NR,NZ),NR=1,NRAX)
70 CONTINUE
WOT6,10
WOT6,80
80 FORMAT(58H INDICES TO IDENTIFY MATERIAL IN EACH REGION OF COLLIMAT
1OR)
DO 90 NZ=1,NZAX
RIT7,40,(MAT2(NR,NZ),NR=1,NRAX)
WOT6,40,(MAT2(NR,NZ),NR=1,NRAX)
90 CONTINUE
WOT6,10
WOT6,120
120 FORMAT(16H SOURCE ENERGIES)
RIT7,130,(ESO(NESO),NESO=1,NESX)
WOT6,130,(ESO(NESO),NESO=1,NESX)
130 FORMAT(10F7.3)
WOT6,10
WOT6,140
140 FORMAT(37H LOWER BOUNDARIES OF VERTICAL REGIONS)
RIT7,150,(ZH(NZ),NZ=1,NZAX)
WOT6,150,(ZH(NZ),NZ=1,NZAX)
150 FORMAT(9F8.2)
WOT6,10
WOT6,160
160 FORMAT(35H INNER BOUNDARIES OF RADIAL REGIONS)
RIT7,150,(RHO(NR),NR=1,NRAX)
WOT6,150,(RHO(NR),NR=1,NRAX)
WOT6,10

```

```

      WOT6,170
170  FORMAT(17H DENSITIES, G/CM3)
      RIT7,180,(DEN(NMAT),NMAT=1,MATX)
      WOT6,180,(DEN(NMAT),NMAT=1,MATX)
180  FORMAT(1P6E11.3)
      WOT6,10
      DO 230 NMAT=1,MATX
      RIT7,190
      WOT6,190
190  FORMAT(72H
1
      WOT6,200
200  FORMAT(24H0ENERGY COMPTON TOTAL)
      DO 220 M=1,MXAX
      RIT7,210,EB(M),DUM1,XSECB(M,1,NMAT),DUM2,DUM3,DUM4,XSECB(M,2,NMAT)
      WOT6,210,EB(M),(XSECB(M,1,NMAT),I=1,2)
210  FORMAT(F7.3,1P7E10.3)
220  CONTINUE
      WOT6,10
230  CONTINUE
      WOT6,240
240  FORMAT(57H LOWER LIMITS ON COSINE THETA FOR ANGULAR CLASSIFICATION
1S)
      RIT7,250,(CTH(NTH),NTH=1,NTHX)
      WOT6,250,(CTH(NTH),NTH=1,NTHX)
250  FORMAT(8F9.5)
      WOT6,10
      WOT6,260
260  FORMAT(40H LOWER LIMITS FOR ENERGY CLASSIFICATIONS)
      RIT7,130,(ECLS(NEC),NEC=1,NEAX)
      WOT6,130,(ECLS(NEC),NEC=1,NEAX)
      WOT6,10
      WOT6,270
270  FORMAT(21H SPLITTING PARAMETERS)
      DO 280 NZ=1,NZAX
      RIT7,40,(NSPL(NR,NZ),NR=1,NRAX)
      WOT6,40,(NSPL(NR,NZ),NR=1,NRAX)
280  CONTINUE
      WOT6,10
      WOT6,290
290  FORMAT(37H SOURCE SAMPLING ANGULAR DISTRIBUTION)
      RIT7,250,(CTHO(NASO),NASO=1,NASX)
      WOT6,250,(CTHO(NASO),NASO=1,NASX)
      RIT7,250,(SOANG(NASO),NASO=1,NASX)
      WOT6,250,(SOANG(NASO),NASO=1,NASX)
      WOT6,10
      WOT6,300
300  FORMAT(22H ENERGY CUTOFF INDICES)
      RIT7,40,(IWCT(NMAT),NMAT=1,MATX)
      WOT6,40,(IWCT(NMAT),NMAT=1,MATX)
      WOT6,10
      RETURN
      END

```

```

C      SUBROUTINE DATEX                      3-2-67
C      EXPANDS INPUT DATA FOR TABLE LOOK-UP AND DOES OTHER PRELIMINARY
C      WORK NEEDED FOR THE MAIN PART OF THE CALCULATION
      SUBROUTINE DATEX
      DIMENSION CPH(360),CTH(20),DEN(4),EB(25),ECLS(30),MAT(10,10),
1     MAT2(10,10),NEREM(50),NPREM(50),NRREM(50),NSPL(10,10),
2     NZREM(50),PART(10,10),RHO(10),RHO2(10),RSO(10),SPEC(20,30),
3     SPEC2(20,30),SPH(360),UC(300,4),UT(300,4),UXREM(50),
4     UYREM(50),UZREM(50),WREM(50),WTREM(50),XREM(50),XSEC(2,4),
5     XSECB(25,2,4),YREM(50),ZH(10),ZREM(50),ZSO(10)
      DIMENSION ESO(2),CTHO(10),SOANG(10),IWCT(4),WMAX(4)
      COMMON CPH,CTH,DEN,EB,ECLS,ESO,IHIX,MAT,MAT2,MATX,MXAX,
1     NE,NEAX,NEREM,NESO,NESX,NPREM,NR,NR1,NRAN,NRAX,NRREM,NRSO,
2     NRSX,NRWL,NSCT,NSEG,NSPL,NTHX,NZ,NZ1,NZAX,NZBT,NZREM,NZSO,
3     NZSX,NZTP,PART,RAN,RHO,RHO2,RSO,S,SPEC,SPEC2,SPH,SUZ,UC,UT,
4     UX,UXREM,UY,UYREM,UZ,UZREM,W,WMAX,WREM,WT,WTREM,X,XN,XREM,
5     XSEC,XSECB,Y,YN,YREM,Z,ZH,ZN,ZREM,ZSO
      COMMON CTHO,IWCT,NASX,SOANG
      NTABIN=1
      DO 10 NRA=1,NRAN
10     RAN=RAM2B(0)
      MXAX2=MXAX/2
      MM=MXAX+1
      DO 15 M=1,MXAX2
      MM=MM-1
      DUM=EB(M)
      EB(M)=EB(MM)
      EB(MM)=DUM
      DO 15 I=1,2
      DO 15 NMAT=1,MATX
      DUM=XSECB(M,I,NMAT)
      XSECB(M,I,NMAT)=XSECB(MM,I,NMAT)
      XSECB(MM,I,NMAT)=DUM
15     CONTINUE
      DO 30 M=1,MXAX
      DO 20 I=1,2
      DO 20 NMAT=1,MATX
      XSECB(M,I,NMAT)=XSECB(M,I,NMAT)*DEN(NMAT)
20     XSECB(M,I,NMAT)=ELOG(XSECB(M,I,NMAT))
30     EB(M)=ELOG(EB(M))
      MATX2=2*MATX
      DO 50 NE=1,300
      E=NE
      E=0.005*E
      E=ELOG(E)
      CALL TABIN(NTABIN,XSECB,EB,MXAX,MATX2,E,XSEC)
      DO 40 NMAT=1,MATX
      UC(NE,NMAT)=EXP(XSEC(1,NMAT))
40     UT(NE,NMAT)=EXP(XSEC(2,NMAT))
50     CONTINUE
      PH=-0.5
      DO 60 IPH=1,360
      PH=PH+1.0
      PHR=PH*0.017453293
      CPH(IPH)=COS(PHR)
60     SPH(IPH)=SIN(PHR)

```

```

      DO 70 NR=1,NRAX
70  RH02(NR)=RHO(NR)**2
      NSPT=NRSX*NZSX
      NSPG=IHIX/NSPT
      IF(NSPG*NSPT-IHIX)80,110,80
80  WOT6,90
90  FORMAT(62H0 NUMBER OF HISTORIES NOT DIVISIBLE BY NUMBER OF SOURCE
      1POINTS)
100 CALL SYSTEM
110 FNRSX=NRSX
      DO 120 NRSO=1,NRSX
      FNRSO=NRSO
120 RSO(NRSO)=0.5*(SQRT(((FNRSX-FNRSO)*RH02(NR1)+FNRSO*RH02(NR1+1))
      1 /FNRSX)+SQRT(((FNRSX-FNRSO+1.0)*RH02(NR1)+(FNRSO-1.0)*RH02(NR1
      2 +1))/FNRSX))
      FNZSX=NZSX
      DO 130 NZSO=1,NZSX
      FNZSO=NZSO
130 ZSO(NZSO)=((2.0*FNZSO-1.0)*ZH(NZ1+1)+(2.0*(FNZSX-FNZSO)+1.0)
      1 *ZH(NZ1))/(2.0*FNZSX)
      NSEG=NSPG/NESX
      IF(NSEG*NESX-NSPG)140,160,140
140 WOT6,150
150 FORMAT(86H0 NUMBER OF HISTORIES FOR EACH SOURCE POINT NOT DIVISIBL
      1E BY NUMBER OF SOURCE ENERGIES)
      GO TO 100
160 DO 170 NR=1,NRAX
      DO 170 NZ=1,NZAX
170 PART(NR,NZ)=NSPL(NR,NZ)
      DO 180 NTH=1,NTHX
      DO 180 NEC=1,NEAX
      SPEC(NTH,NEC)=0.0
180 SPEC2(NTH,NEC)=0.0
      DO 190 NMAT=1,MATX
      NEC=IWCT(NMAT)
190 WMAX(NMAT)=0.511/ECLS(NEC)
      RETURN
      END

```

```

$      FASTRAN
C      SUBROUTINE TRACK                      3-13-67
C      GENERATES PHOTON HISTORIES
C      S'ROUTINE TRACK
      DIMENSION CPH(360),CTH(20),DEN(4),EB(25),ECLS(30),MAT(10,10),
      1  MAT2(10,10),NEREM(50),NPREM(50),NRREM(50),NSPL(10,10),
      2  NZREM(50),PART(10,10),RHO(10),RHO2(10),RSO(10),SPEC(20,30),
      3  SPEC2(20,30),SPH(360),UC(300,4),UT(300,4),UXREM(50),
      4  UYREM(50),UZREM(50),WREM(50),WTREM(50),XREM(50),XSEC(2,4),
      5  XSECB(25,2,4),YREM(50),ZH(10),ZREM(50),ZSO(10)
      DIMENSION ESO(2),CTHO(10),SOANG(10),IWCT(4),WMAX(4)
      COMMON CPH,CTH,DEN,EB,ECLS,ESO,IHIX,MAT,MAT2,MATX,MXAX,
      1  NE,NEAX,NEREM,NESO,NESX,NPREM,NR,NR1,NRAN,NRAX,NRREM,NRSO,
      2  NRSX,NRWL,NSCT,NSEG,NSPL,NTHX,NZ,NZ1,NZAX,NZBT,NZREM,NZSO,
      3  NZSX,NZTP,PART,RAN,RHO,RHO2,RSO,S,SPEC,SPEC2,SPH,SUZ,UC,UT,
      4  UX,UXREM,UY,UYREM,UZ,UZREM,W,WMAX,WREM,WT,WTREM,X,XN,XREM,

```

```

5  XSEC,XSECB,Y,YN,YREM,Z,ZH,ZN,ZREM,ZSO
COMMON CTHO,IWCT,NASX,SOANG
DIMENSION SUZREM(50)
ISPL=0
X=RSO(NRSO)
Y=0.0
Z=ZSO(NZSO)
W=0.511/ESO(NESO)
RAN=RAM2B(0)
DO 2 NASO=2,NASX
NA=NASO
IF (RAN-SOANG(NASO)) 4,2,2
2 CONTINUE
4 RAN=RAM2B(0)
DCTH=CTHO(NA)-CTHO(NA-1)
UZ=CTHO(NA-1)+RAN*DCTH
WT=DCTH/((SOANG(NA)-SOANG(NA-1))*2.0)
RAN=RAM2B(0)
IPH=360.0*RAN
SUZ=SQRT(1.0-UZ**2)
UX=SUZ*CPH(IPH+1)
UY=SUZ*SPH(IPH+1)
NR=NR1
NZ=NZ1
NE=102.2/W+0.5
10 NMAT=MAT(NR,NZ)
RAN=RAM2B(0)
NE=NE
S=-ELOG(RAN)/UT(NE,NMAT)
XN=UX*S+X
YN=UY*S+Y
ZN=UZ*S+Z
CALL CHECK
X=XN
Y=YN
Z=ZN
NR=NR
NZ=NZ
IF (MAT(NR,NZ)) 80,20,30
20 CALL VACUO
NR=NR
NZ=NZ
IF (MAT(NR,NZ)) 80,30,30
30 IF (NSCT) 10,10,40
40 IF (NSPL(NR,NZ)) 60,60,50
50 ISPL=ISPL+1
IF (ISPL-50) 55,55,60
55 WT=WT/PART(NR,NZ)
NPREM(ISPL)=NSPL(NR,NZ)-1
XREM(ISPL)=X
YREM(ISPL)=Y
ZREM(ISPL)=Z
UXREM(ISPL)=UX
UYREM(ISPL)=UY
UZREM(ISPL)=UZ
SUZREM(ISPL)=SUZ

```



```

      WREM( ISPL )=W
      NEREM( ISPL )=NE
      WTREM( ISPL )=WT
      NRREM( ISPL )=NR
      NZREM( ISPL )=NZ
60  NE=NE
      NMAT=MAT( NR,NZ )
      NMATR=MAT2( NR,NZ )
      DIFAT=UT( NE,NMAT )-UT( NE,NMATR )
      DENOM=DIFAT+UC( NE,NMATR )
      RAN=RAM2B( 0 )
      IF( RAN-DENOM/UT( NE,NMAT ) ) 65,65,100
65  RAN=RAM2B( 0 )
      IF( RAN-DIFAT/DENOM ) 10,70,70
70  CALL COMPT2
      NMAT=MAT2( NR,NZ )
      IF( W=WMAX( NMAT ) ) 10,100,100
80  IF( MAT( NR,NZ )+1 ) 90,100,100
90  CALL GRADE
100 IF( ISPL ) 140,140,110
110 IF( NPREM( ISPL ) ) 120,120,130
120 ISPL=ISPL-1
      GO TO 100
130 NPREM( ISPL )=NPREM( ISPL )-1
      X=XREM( ISPL )
      Y=YREM( ISPL )
      Z=ZREM( ISPL )
      UX=UXREM( ISPL )
      UY=UYREM( ISPL )
      UZ=UZREM( ISPL )
      SUZ=SUZREM( ISPL )
      W=WREM( ISPL )
      NE=NEREM( ISPL )
      WT=WTREM( ISPL )
      NR=NRREM( ISPL )
      NZ=NZREM( ISPL )
      GO TO 60
140 RETURN
      END

```

```

$      FASTRAN
C      SUBROUTINE CHECK                      3-2-67
C      CHECKS TO SEE IF BOUNDARY HAS BEEN CROSSED
      SUBROUTINE CHECK
      DIMENSION CPH(360),CTH(20),DEN(4),EB(25),ECLS(30),MAT(10,10),
1  MAT2(10,10),NEREM(50),NPREM(50),NRREM(50),NSPL(10,10),
2  NZREM(50),PART(10,10),RHO(10),RHO2(10),RSO(10),SPEC(20,30),
3  SPEC2(20,30),SPH(360),UC(300,4),UT(300,4),UXREM(50),
4  UYREM(50),UZREM(50),WREM(50),WTREM(50),XREM(50),XSEC(2,4),
5  XSECB(25,2,4),YREM(50),ZH(10),ZREM(50),ZSO(10)
      DIMENSION ESO(2),CTHO(10),SOANG(10),IWCT(4),WMAX(4)
      COMMON CPH,CTH,DEN,EB,ECLS,ESO,IHIX,MAT,MAT2,MATX,MXAX,
1  NE,NEAX,NEREM,NEOX,NEOX,NPREM,NR,NR1,NRAN,NRAX,NRREM,NRSD,
2  NRSD,NRWL,NSCT,NSEG,NSPL,NTHX,NZ,NZ1, NZAX,NZBT,NZREM,NZSO,
3  NZSD,NZTP,PART,RAN,RHO,RHO2,RSO,S,SPEC,SPEC2,SPH,SUZ,UC,UT:

```

```

4  UX,UXREM,UY,UYREM,UZ,UZREM,W,WMAX,WREM,WT,WTREM,X,XN,XREM,
5  XSEC,XSECB,Y,YN,YREM,Z,ZH,ZN,ZREM,ZSO
COMMON CTHO,IWCT,NASX,SOANG
DRAD=X*UX+Y*UY
IF(DRAD)200,10,10
10 IF(UZ)130,100,20
20 IF(ZN-ZH(NZ+1))100,30,30
30 SB=(ZH(NZ+1)-Z)/UZ
X1=SB*UX+X
Y1=SB*UY+Y
40 IF(X1**2+Y1**2-RHO2(NR+1))90,70,50
50 NR=NR+1
IF(MAT(NR,NZ)-MAT(NR-1,NZ))60,40,60
60 IF(MAT(NR,NZ))480,65,65
65 SUZ2=UX**2+UY**2
SB=(SQRT(DRAD**2-SUZ2*(X**2+Y**2-RHO2(NR)))-DRAD)/SUZ2
ZN=SB*UZ+Z
XN=SB*UX+X
YN=SB*UY+Y
NSGT=0
GO TO 480
70 NR=NR+1
NZ=NZ+1
IF(MAT(NR,NZ)-MAT(NR-1,NZ-1))80,20,80
80 IF(MAT(NR,NZ))480,85,85
85 ZN=ZH(NZ)
XN=X1
YN=Y1
NSGT=0
GO TO 480
90 NZ=NZ+1
IF(MAT(NR,NZ)-MAT(NR,NZ-1))80,20,80
100 IF(XN**2+YN**2-RHO2(NR+1))120,110,110
110 NR=NR+1
IF(MAT(NR,NZ)-MAT(NR-1,NZ))60,100,60
120 NSGT=1
GO TO 480
130 IF(ZH(NZ)-ZN)100,140,140
140 SB=(ZH(NZ)-Z)/UZ
X1=SB*UX+X
Y1=SB*UY+Y
150 IF(X1**2+Y1**2-RHO2(NR+1))190,170,160
160 NR=NR+1
IF(MAT(NR,NZ)-MAT(NR-1,NZ))60,150,60
170 NR=NR+1
NZ=NZ-1
IF(MAT(NR,NZ)-MAT(NR-1,NZ+1))180,130,180
180 IF(MAT(NR,NZ))480,185,185
185 ZN=ZH(NZ+1)
XN=X1
YN=Y1
NSGT=0
GO TO 480
190 NZ=NZ-1
IF(MAT(NR,NZ)-MAT(NR,NZ+1))180,130,180
200 SUZ2=UX**2+UY**2

```

```

      SM=-DRAD/SUZ2
      DS=S-SM
      IF(DS)220,220,210
210  XM=UX*SM+X
      YM=UY*SM+Y
      ZM=UZ*SM+Z
      GO TO 230
220  XM=XN
      YM=YN
      ZM=ZN
230  IF(UZ)390,340,240
240  IF(ZM-ZH(NZ+1))340,250,250
250  SB=(ZH(NZ+1)-Z)/UZ
      X1=SB*UX+X
      Y1=SB*UY+Y
260  IF(X1**2+Y1**2-RHO2(NR))320,290,270
270  NZ=NZ+1
      IF(MAT(NR,NZ)-MAT(NR,NZ-1))280,240,280
280  IF(MAT(NR,NZ))480,285,285
285  ZN=ZH(NZ)
      XN=X1
      YN=Y1
      NSCT=0
      GO TO 480
290  NR=NR-1
      IF(NR)300,300,310
300  NR=NR+1
      GO TO 270
310  NZ=NZ+1
      IF(MAT(NR,NZ)-MAT(NR+1,NZ-1))280,240,280
320  NR=NR-1
      IF(MAT(NR,NZ)-MAT(NR+1,NZ))330,260,330
330  IF(MAT(NR,NZ))480,335,335
335  SB=(-DRAD-SQRT(DRAD**2-SUZ2*(X**2+Y**2-RHO2(NR+1))))/SUZ2
      XN=SB*UX+X
      YN=SB*UY+Y
      ZN=SB*UZ+Z
      NSCT=0
      GO TO 480
340  IF(XM**2+YM**2-RHO2(NR))380,350,350
350  IF(DS)370,370,360
360  X=XM
      Y=YM
      Z=ZM
      DRAD=X*UX+Y*UY
      GO TO 10
370  XN=XM
      YN=YM
      ZN=ZM
      NSCT=1
      GO TO 480
380  NR=NR-1
      IF(MAT(NR,NZ)-MAT(NR+1,NZ))330,340,330
390  IF(ZH(NZ)-ZM)340,400,400
400  SB=(ZH(NZ)-Z)/UZ
      X1=SB*UX+X

```

```

      Y1=SB*UY+Y
410 IF (X1**2+Y1**2-RHO2(NR)) 470,440,420
420 NZ=NZ-1
      IF (MAT(NR,NZ)-MAT(NR,NZ+1)) 430,390,430
430 IF (MAT(NR,NZ)) 480,435,435
435 ZN=ZH(NZ+1)
      XN=X1
      YN=Y1
      NSCT=0
      GO TO 480
440 NR=NR-1
      IF (NR) 450,450,460
450 NR=NR+1
      GO TO 420
460 NZ=NZ-1
      IF (MAT(NR,NZ)-MAT(NR+1,NZ+1)) 430,390,430
470 NR=NR-1
      IF (MAT(NR,NZ)-MAT(NR+1,NZ)) 330,410,330
480 RETURN
      END

```

```

$      FASTRAN
C      SUBROUTINE VACUO                      3-2-67
C      MOVES PHOTON FROM POSITION IN HOLE TO WALL OR FLOOR OF COLLIMATOR
C      OR TO DETECTOR
      SUBROUTINE VACUO
      DIMENSION CPH(360),CTH(20),DEN(4),EB(25),ECLS(30),MAT(10,10),
1  MAT2(10,10),NEREM(50),NPREM(50),NRREM(50),NSPL(10,10),
2  NZREM(50),PART(10,10),RHO(10),RHO2(10),RSO(10),SPEC(20,30),
3  SPEC2(20,30),SPH(360),UC(300,4),UT(300,4),UXREM(50),
4  JYREM(50),UZREM(50),WREM(50),WTREM(50),XREM(50),XSEC(2,4),
5  XSECB(25,2,4),YREM(50),ZH(10),ZREM(50),ZSO(10)
      DIMENSION ESO(2),CTHO(10),SOANG(10),IWCT(4),WMAX(4)
      COMMON CPH,CTH,DEN,EB,ECLS,ESO,IHIX,MAT,MAT2,MATX,MXAX,
1  NE,NEAX,NEREM,NESO,NESX,NPREM,NR,NR1,NRAN,NRAX,NRREM,NRSO,
2  NRSX,NRWL,NSCT,NSEG,NSPL,NTHX,NZ,NZ1,NZAX,NZBT,NZREM,NZSO,
3  NZSX,NZTP,PART,RAN,RHO,RHO2,RSO,S,SPEC,SPEC2,SPH,SUZ,UC,UT,
4  UX,UXREM,UY,UYREM,UZ,UZREM,W,WMAX,WREM,WT,WTREM,X,XN,XREM,
5  XSEC,XSECB,Y,YN,YREM,Z,ZH,ZN,ZREM,ZSO
      COMMON CTHO,IWCT,NASX,SOANG
      IF (UZ) 110,70,10
10 SB=(ZH(NZTP)-Z)/UZ
      ZN=ZH(NZTP)
      XN=UX*SB+X
      YN=UY*SB+Y
      R2=XN**2+YN**2
      NZ=NZTP
      IF (R2-RHO2(NRWL)) 30,20,70
20 NR=NRWL
      GO TO 120
30 DO 40 NRC=1,NRWL
      NR=NRC
      IF (R2-RHO2(NRC)) 60,50,40
40 CONTINUE
50 IF (UX*XN+UY*YN) 60,120,120

```

```

60 NR=NR-1
   GO TO 120
70 NR=NRWL
   DRAD=UX*X+UY*Y
   SUZ2=UX**2+UY**2
   SB=(SQRT(DRAD**2-SUZ2*(X**2+Y**2-RHO2(NRWL)))-DRAD)/SUZ2
   XN=UX*SB+X
   YN=UY*SB+Y
   ZN=UZ*SB+Z
   DO 80 NZC=NZBT,NZTP
   NZ=NZC
   IF(ZN-ZH(NZC))100,90,80
80 CONTINUE
90 IF(UZ)100,120,120
100 NZ=NZ-1
   GO TO 120
110 SB=(ZH(NZBT)-Z)/UZ
   ZN=ZH(NZBT)
   XN=SB*UX+X
   YN=SB*UY+Y
   R2=XN**2+YN**2
   NZ=NZBT-1
   IF(R2-RHO2(NRWL))30,20,70
120 X=XN
   Y=YN
   Z=ZN
   NSCT=0
   RETURN
   END

```

```

$      FASTRAN
C      SUBROUTINE COMPT2                      3-2-67
C      SAMPLE NEW DIRECTION AND ENERGY FROM COMPTON DISTRIBUTION
      SUBROUTINE COMPT2
        DIMENSION CPH(360),CTH(20),DEN(4),EB(25),ECLS(30),MAT(10,10),
1       MAT2(10,10),NEREM(50),NPREM(50),NRREM(50),NSPL(10,10),
2       NZREM(50),PART(10,10),RHO(10),RHO2(10),RSO(10),SPEC(20,30),
3       SPEC2(20,30),SPH(360),UC(300,4),UT(300,4),UXREM(50),
4       UYREM(50),UZREM(50),WREM(50),WTREM(50),XREM(50),XSEC(2,4),
5       XSECB(25,2,4),YREM(50),ZH(10),ZREM(50),ZSO(10)
        DIMENSION ESO(2),CTHO(10),SOANG(10),IWCT(4),WMAX(4)
        COMMON CPH,CTH,DEN,EB,ECLS,ESO,IHIX,MAT,MAT2,MATX,MXAX,
1       NE,NEAX,NEREM,NESO,NESX,NPREM,NR,NR1,NRAN,NRAX,NRREM,NRSO,
2       NRSX,NRWL,NSCT,NSEG,NSPL,NTHX,NZ,NZ1,NZAX,NZBT,NZREM,NZSO,
3       NZSX,NZTP,PART,RAN,RHO,RHO2,RSO,S,SPEC,SPEC2,SPH,SUZ,UC,UT,
4       UX,UXREM,UY,UYREM,UZ,UZREM,W,WMAX,WREM,WT,WTREM,X,XN,XREM,
5       XSEC,XSECB,Y,YN,YREM,Z,ZH,ZN,ZREM,ZSO
        COMMON CTHO,IWCT,NASX,SOANG
10      RAN=RAM2B(0)
        T=2.0/W
        IF(RAN-(1.0+T)/(9.0+T))20,20,30
20      RAN=RAM2B(0)
        R=1.0+RAN*T
        RAN=RAM2B(0)
        IF(RAN-4.0*(R-1.0)/(R**2))40,40,10

```

```

30 RAN=RAM2B(0)
   R=(1.0+T)/(1.0+RAN*T)
   RAN=RAM2B(0)
   IF (RAN-0.5*((W-R*W+1.0)**2+1.0/R))40,40,10
40 WN=W*R
   COM=1.0+W-WN
   W=WN
   NMAT=MAT2(NR,NZ)
   IF (W-WMAX(NMAT))45,80,80
45 SOM=SQRT(1.0-COM**2)
   NE=102.2/W+0.5
   RAN=RAM2B(0)
   IPH=360.0*RAN
   UZN=UZ*COM+SUZ*SOM*CPH(IPH+1)
   SUZN=SQRT(1.0-UZN**2)
   A=SUZ*SUZN
   IF (A-0.000001)50,50,60
50 UXN=-CPH(IPH+1)*SUZN
   UYN=SPH(IPH+1)*SUZN
   GO TO 70
60 CDPH=(COM-UZ*UZN)/A
   SDPH=SOM*SPH(IPH+1)/SUZN
   UXN=((UX*CDPH-UY*SDPH)*SUZN)/SUZ
   UYN=((UY*CDPH+UX*SDPH)*SUZN)/SUZ
70 UX=UXN
   UY=UYN
   UZ=UZN
   SUZ=SUZN
80 RETURN
   END

```

```

$      FASTRAN
C      SUBROUTINE GRADE          3-2-67
C      RECORDS SCORE WHEN PHOTON ENTERS DETECTOR
      SUBROUTINE GRADE
        DIMENSION CPH(360),CTH(20),DEN(4),EB(25),ECLS(30),MAT(10,10),
1       MAT2(10,10),NEREM(50),NPREM(50),NRREM(50),NSPL(10,10),
2       NZREM(50),PART(10,10),RHO(10),RHO2(10),RSO(10),SPEC(20,30),
3       SPEC2(20,30),SPH(360),UC(300,4),UT(300,4),UXREM(50),
4       UYREM(50),UZREM(50),WREM(50),WTREM(50),XREM(50),XSEC(2,4),
5       XSECB(25,2,4),YREM(50),ZH(10),ZREM(50),ZSO(10)
        DIMENSION ESO(2),CTHO(10),SOANG(10),IWCT(4),WMAX(4)
        COMMON CPH,CTH,DEN,EB,ECLS,ESO,IHIX,MAT,MAT2,MATX,MXAX,
1       NE,NEAX,NEREM,NESE,NESX,NPREM,NR,NR1,NRAN,NRAX,NRREM,NRSO,
2       NRSX,NRWL,NSCT,NSEG,NSPL,NTHX,NZ,NZ1,NZAX,NZBT,NZREM,NZSO,
3       NZSX,NZTP,PART,RAN,RHO,RHO2,RSO,S,SPEC,SPEC2,SPH,SUZ,UC,UT,
4       UX,UXREM,UY,UYREM,UZ,UZREM,W,WMAX,WREM,WT,WTREM,X,XN,XREM,
5       XSEC,XSECB,Y,YN,YREM,Z,ZH,ZN,ZREM,ZSO
        COMMON CTHO,IWCT,NASX,SOANG
        DO 10 NTH=1,NTHX
          JTH=NTH
          IF (UZ-CTH(NTH))10,20,20
10      CONTINUE
20      E=0.511/W
        DO 30 NEC=1,NEAX

```

```

      NECL=NEC
      IF (E-ECLS(NEC)) 30,40,40
30  CONTINUE
40  SPEC(JTH,NECL)=SPEC(JTH,NECL)+WT
      SPEC2(JTH,NECL)=SPEC2(JTH,NECL)+WT**2
      RETURN
      END

```

```

$      FASTRAN
C      SUBROUTINE TEACH                      4-20-67
C      NORMALIZES AND PRINTS RESULTS
      SUBROUTINE TEACH
      DIMENSION CPH(360),CTH(20),DEN(4),EB(25),ECLS(30),MAT(10,10),
1  MAT2(10,10),NEREM(50),NPREM(50),NRREM(50),NSPL(10,10),
2  NZREM(50),PART(10,10),RHO(10),RHO2(10),RSO(10),SPEC(20,30),
3  SPEC2(20,30),SPH(360),UC(300,4),UT(300,4),UXREM(50),
4  UYREM(50),UZREM(50),WREM(50),WTREM(50),XREM(50),XSEC(2,4),
5  XSECB(25,2,4),YREM(50),ZH(10),ZREM(50),ZSO(10)
      DIMENSION ESO(2),CTHO(10),SOANG(10),IWCT(4),WMAX(4)
      COMMON CPH,CTH,DEN,EB,ECLS,ESO,IHIX,MAT,MAT2,MATX,MXAX,
1  NE,NEAX,NEREM,NESO,NESX,NPREM,NR,NR1,NRAN,NRAX,NRREM,NRSO,
2  NRSX,NRWL,NSCT,NSEG,NSPL,IJTHX,NZ,NZ1,NZAX,NZBT,NZREM,NZSO,
3  NZSX,NZTP,PART,RAN,RHO,RHO2,RSO,S,SPEC,SPEC2,SPH,SUZ,UC,UT,
4  UX,UXREM,UY,UYREM,UZ,UZREM,W,WMAX,WREM,WT,WTREM,X,XN,XREM,
5  XSEC,XSECB,Y,YN,YREM,Z,ZH,ZN,ZREM,ZSO
      COMMON CTHO,IWCT,NASX,SOANG,LP
      DIMENSION ASPEC(20),ASPEC2(20),ESPEC(30),ESPEC2(30)
      WOT6,10
10  FORMAT(1H0)
      FLP=LP
      HIX=IHIX
      HIX=HIX*FLP
      DO 11 NEC=1,NEAX
      ESPEC(NEC)=0.0
      ESPEC2(NEC)=0.0
      DO 11 NTH=1,NTHX
      ESPEC(NEC)=ESPEC(NEC)+SPEC(NTH,NEC)
11  ESPEC2(NEC)=ESPEC2(NEC)+SPEC2(NTH,NEC)
      DO 12 NTH=1,NTHX
      ASPEC(NTH)=0.0
      ASPEC2(NTH)=0.0
      DO 12 NEC=1,NEAX
      ASPEC(NTH)=ASPEC(NTH)+SPEC(NTH,NEC)
12  ASPEC2(NTH)=ASPEC2(NTH)+SPEC2(NTH,NEC)
      DO 15 NTH=1,NTHX
      ASPEC(NTH)=ASPEC(NTH)/HIX
      ASPEC2(NTH)=ASPEC2(NTH)/HIX
      ASPEC2(NTH)=(ASPEC2(NTH)-ASPEC(NTH)**2)/(HIX-1.0)
      IF(ASPEC(NTH))13,14,13
13  ASPEC2(NTH)=SQRT(ASPEC2(NTH))/ASPEC(NTH)
      GO TO 15
14  ASPEC2(NTH)=-10.0
15  CONTINUE
      DO 18 NEC=1,NEAX
      ESPEC(NEC)=ESPEC(NEC)/HIX

```

```

      ESPEC2(NEC)=ESPEC2(NEC)/HIX
      ESPEC2(NEC)=(ESPEC2(NEC)-ESPEC(NEC)**2)/(HIX-1.0)
      IF(ESPEC(NEC))16,17,16
16    ESPEC2(NEC)=SQRT(ESPEC2(NEC))/ESPEC(NEC)
      GO TO 18
17    ESPEC2(NEC)=-10.0
18    CONTINUE
      DO 40 NTH=1,NTHX
      DO 40 NEC=1,NEAX
      SPEC(NTH,NEC)=SPEC(NTH,NEC)/HIX
      SPEC2(NTH,NEC)=SPEC2(NTH,NEC)/HIX
      SPEC2(NTH,NEC)=(SPEC2(NTH,NEC)-SPEC(NTH,NEC)**2)/(HIX-1.0)
      IF(SPEC(NTH,NEC))20,30,20
20    SPEC2(NTH,NEC)=SQRT(SPEC2(NTH,NEC))/SPEC(NTH,NEC)
      GO TO 40
30    SPEC2(NTH,NEC)=-10.0
40    CONTINUE
      WOT6,50
50    FORMAT(46H ENERGY-ANGLE SPECTRA EMERGING FROM COLLIMATOR)
      WOT6,60
60    FORMAT(65H CTH IS THE COSINE OF THE LARGEST ANGLE IN GIVEN ANGULAR
      { INTERVAL)
      WOT6,70
70    FORMAT(49H ECLS IS SMALLEST ENERGY IN GIVEN ENERGY INTERVAL)
      WOT6,80
80    FORMAT(46H DATA ARE NORMALIZED TO ONE PHOTON FROM SOURCE)
      WOT6,10
      IF(NEAX-10)84,84,82
82    NBOT=1
      NTOP=10
      GO TO 86
84    NBOT=1
      NTOP=NEAX
86    WOT6,90,(ECLS(NEC),NEC=NBOT,NTOP)
90    FORMAT(12H CTH, ECLS=F7.3,9F10.3)
      WOT6,10
      DO 110 NTH=1,NTHX
      WOT6,100,(CTH(NTH),(SPEC(NTH,NEC),NEC=NBOT,NTOP)
100    FORMAT(F7.3,1PE14.2,1P9E10.2)
110    CONTINUE
      WOT6,10
      WOT6,111,(ESPEC(NEC),NEC=NBOT,NTOP)
111    FORMAT(7H SUM 1PE14.2,1P9E10.2)
      WOT6,10
      IF(NEAX-NTOP)116,116,112
112    NBOT=NTOP+1
      NTOP=NTOP+10
      IF(NEAX-NTOP)114,86,86
114    NTOP=NEAX
      GO TO 86
116    WOT6,120
120    FORMAT(59H FRACTIONAL STATISTICAL DEVIATION OF SPECTRA IN ABOVE TA
      BLE)
      WOT6,10
      IF(NEAX-10)124,124,122
122    NBOT=1

```



```

      NTOP=10
      GO TO 126
124 NBOT=1
      NTOP=NEAX
126 WOT6,90,(ECLS(NEC),NEC=NBOT,NTOP)
      WOT6,10
      DO 130 NTH=1,NTHX
      WOT6,140,CTH(NTH),(SPEC2(NTH,NEC),NEC=NBOT,NTOP)
130 CONTINUE
140 FORMAT(F7.3,F14.4,9F10.4)
      WOT6,10
      WOT6,141,(ESPEC2(NEC),NEC=NBOT,NTOP)
141 FORMAT(10H SUM DEV. F11.4,9F10.4)
      WOT6,10
      IF(NEAX-NTOP)146,146,142
142 NBOT=NTOP+1
      NTOP=NTOP+10
      IF(NEAX-NTOP)144,126,126
144 NTOP=NEAX
      GO TO 126
146 WOT6,150
150 FORMAT(30H          ANGULAR          FRACTIONAL)
      WOT6,160
160 FORMAT(29H CTH DISTRIBUTION DEVIATION)
      DO 170 NTH=1,NTHX
      WOT6,180,CTH(NTH),ASPEC(NTH),ASPEC2(NTH)
170 CONTINUE
180 FORMAT(F7.3,1PE12.2,0PF11.4)
      WOT6,10
      RETURN
      END

```

```

$      FASTRAN
C      SUBROUTINE TABIN          28-8-64
      SUBROUTINE TABIN(NTABIN,FB,XB,NMAX,MMAX,X,FX)
      DIMENSION FB(25,8),XB(25),FX(8),XBAV(25),D1(25),D2(25)
      GO TO (10,30),NTABIN
10  NMAX1=NMAX-1
      DO 20 N=2,NMAX1
      XBAV(N)=(XB(N-1)+XB(N))/2.0
      D1(N)=(XB(N-1)-XB(N))*(XB(N-1)-XB(N+1))
20  D2(N)=(XB(N)-XB(N-1))*(XB(N)-XB(N+1))
      NTABIN=2
      NEXS=NMAX1-2
30  IF(X-XB(1))60,50,40
40  NX=2
      GO TO 200
50  NX=1
      GO TO 220
60  IF(X-XB(2))80,70,40
70  NX=2
      GO TO 220
80  IF(NEXS)90,110,140
90  WOT6,100
100 FORMAT(33H0NOT ENOUGH BASE POINTS FOR TABIN)

```

```
CALL SYSTEM
110 IF(X-XB(NMAX))130,120,130
120 NX=NMAX
GO TO 220
130 NX=NMAX1
GO TO 200
140 DO 170 N=3,NMAX1
IF(X-XB(N))170,150,160
150 NX=N
GO TO 220
160 NX=N
GO TO 180
170 CONTINUE
GO TO 110
180 IF(X-XBAV(NX))200,200,190
190 NX=NX-1
200 WT1=(X-XB(NX))*(X-XB(NX+1))/D1(NX)
WT2=(X-XB(NX-1))*(X-XB(NX+1))/D2(NX)
WT3=1.0-WT1-WT2
DO 210 M=1,MMAX
210 FX(M)=WT1*FB(NX-1,M)+WT2*FB(NX,M)+WT3*FB(NX+1,M)
RETURN
220 DO 230 M=1,MMAX
230 FX(M)=FB(NX,M)
RETURN
END
```

COLLIMATOR RUN 23, COLLIMATED COBALT SOURCE, PRODUCTION, 4-24-67

NRAN	NEAX	NTHX	MXAX	MATX	NRAX	NZAX	NZTP	NRVL	NZBT	IHX	LP
1000	13	3	25	3	6	6	6	4	5	10000	100

NESX	NRSX	NZSX	NZ1	NZ1	NASX
2	10	5	1	3	2

INDICES TO IDENTIFY PSEUDO-MATERIAL IN EACH REGION OF COLLIMATOR

-1	-1	-1	-1	-1	-1
2	2	-1	-1	-1	-1
2	2	-1	-1	-1	-1
2	2	-1	-1	-1	-1
0	0	0	3	3	-1
-2	-2	-2	-2	-2	-2

INDICES TO IDENTIFY MATERIAL IN EACH REGION OF COLLIMATOR

0	0	0	0	0	0
1	1	0	0	0	0
2	1	0	0	0	0
1	1	0	0	0	0
0	0	0	1	3	0
0	0	0	0	0	0

SOURCE ENERGIES
1.330 1.170

LOWER BOUNDARIES OF VERTICAL REGIONS
-100.00 .00 5.60 5.90 6.00 27.27

INNER BOUNDARIES OF RADIAL REGIONS
.00 .50 .60 1.27 1.43 2.43

DENSITIES, G/CM3
7.860E 00 8.710E 00 1.143E 01

MACROSCOPIC X-SECTION DATA FOR FE (UNIT-CH-2/G) PROCESSED ON 2/4/67

ENERGY	COMPTON	TOTAL
.010	1.795E-01	1.716E-02
.015	1.763E-01	5.569E-01
.020	1.732E-01	2.508E-01
.030	1.674E-01	7.875E-00
.040	1.621E-01	3.461E-00
.050	1.574E-01	1.839E-00
.060	1.529E-01	1.127E-00
.080	1.450E-01	5.503E-01
.100	1.381E-01	3.418E-01
.150	1.245E-01	1.838E-01
.200	1.139E-01	1.391E-01
.300	9.905E-02	1.066E-01
.400	8.875E-02	9.208E-02
.500	8.103E-02	8.286E-02
.600	7.496E-02	7.612E-02
.800	6.584E-02	6.643E-02
1.000	5.919E-02	5.956E-02
1.500	4.808E-02	4.860E-02
2.000	4.102E-02	4.249E-02
3.000	3.225E-02	3.611E-02
4.000	2.696E-02	3.309E-02
5.000	2.328E-02	3.146E-02
6.000	2.058E-02	3.055E-02
8.000	1.684E-02	2.987E-02
10.000	1.434E-02	2.989E-02

COBALT, 2-21-67, MACROSCOPIC CROSS-SECTION, CM2/G

ENERGY	COMPTON	TOTAL
.010	1.767E-01	1.866E-02
.015	1.735E-01	6.082E-01
.020	1.706E-01	2.737E-01
.030	1.648E-01	8.667E-00
.040	1.596E-01	3.816E-00
.050	1.550E-01	2.025E-00
.060	1.505E-01	1.239E-00
.080	1.427E-01	5.965E-01
.100	1.360E-01	3.646E-01
.150	1.224E-01	1.893E-01
.200	1.122E-01	1.404E-01

.300	9.751E-02	1.060E-01
.400	8.738E-02	9.114E-02
.500	7.978E-02	8.184E-02
.600	7.380E-02	7.510E-02
.800	6.482E-02	6.549E-02
1.000	5.828E-02	5.869E-02
1.500	4.733E-02	4.789E-02
2.000	4.038E-02	4.191E-02
3.000	3.175E-02	3.570E-02
4.000	2.654E-02	3.282E-02
5.000	2.292E-02	3.128E-02
6.000	2.026E-02	3.044E-02
8.000	1.658E-02	2.988E-02
10.000	1.412E-02	2.938E-02

MACROSCOPIC X-SECTION DATA FOR PB (UNIT=CM**2/G) PROCESSED ON 2/4/67		
ENERGY	COMPTON	TOTAL
.010	1.526E-01	1.321E-02
.015	1.499E-01	1.118E-02
.020	1.473E-01	8.343E-03
.030	1.424E-01	2.790E-03
.040	1.379E-01	1.305E-03
.050	1.338E-01	7.172E-04
.060	1.301E-01	4.470E-04
.080	1.233E-01	2.117E-04
.100	1.174E-01	5.617E-05
.150	1.057E-01	1.987E-05
.200	9.689E-02	9.690E-06
.300	8.424E-02	3.851E-06
.400	7.547E-02	2.208E-06
.500	6.892E-02	1.538E-06
.600	6.375E-02	1.126E-06
.800	5.599E-02	8.558E-07
1.000	5.035E-02	6.832E-07
1.500	4.090E-02	5.092E-07
2.000	3.488E-02	4.498E-07
3.000	2.743E-02	4.155E-07
4.000	2.243E-02	4.146E-07
5.000	1.981E-02	4.237E-07
6.000	1.750E-02	4.345E-07
8.000	1.432E-02	4.601E-07
10.000	1.219E-02	4.869E-07

LOWER LIMITS ON COSINE THETA FOR ANGULAR CLASSIFICATIONS

.99600 .96100 .00000

LOWER LIMITS FOR ENERGY CLASSIFICATIONS

1.300 1.200 1.100 1.000 .900 .800 .700 .600 .500 .400
.300 .200 .100

SPLITTING PARAMETERS

0 0 0 0 0 0 0 0
0 0 0 0 0 0 0 0
0 0 0 0 0 0 0 0
0 0 0 0 0 0 0 0
0 0 0 0 0 0 0 0

SOURCE SAMPLING ANGULAR DISTRIBUTION

-1.00000 1.00000
.00000 1.00000

ENERGY CUTOFF INDICES

13 12

ENERGY-ANGLE SPECTRA EMERGING FROM COLLIMATOR
C_{TH} IS THE COSINE OF THE LARGEST ANGLE IN GIVEN ANGULAR INTERVAL
E_{CLS} IS SMALLEST ENERGY IN GIVEN ENERGY INTERVAL
DATA ARE NORMALIZED TO ONE PHOTON FROM SOURCE

C_{TH}, E_{CLS}= 1.300 1.200 1.100 1.000 .900 .800 .700 .600 .500 .400

.996 4.93E-04 3.00E-06 4.55E-04 1.30E-05 6.00E-06 1.10E-05 1.40E-05 1.20E-05 1.90E-05 2.20E-05
.961 7.00E-06 1.80E-05 3.10E-05 3.60E-05 1.70E-05 8.00E-06 4.00E-06 9.00E-06 8.00E-06 3.00E-06
.000 .00E 00 1.00E-06 8.00E-06 2.60E-05 1.90E-05 2.50E-05 1.90E-05 1.40E-05 1.40E-05

SUM 5.00E-04 2.20E-05 4.54E-04 7.50E-05 4.20E-05 4.40E-05 3.70E-05 3.50E-05 4.10E-05 3.90E-05

UNCLASSIFIED

Security Classification

DOCUMENT CONTROL DATA - R & D

Security classification of title, body of abstract and indexing annotation must be entered when the overall report is classified

1. ORIGINATING ACTIVITY (Corporate author) University of Illinois Urbana, Illinois		2a. REPORT SECURITY CLASSIFICATION Unclassified	
		2b. GROUP	
3. REPORT TITLE MONTE CARLO CALCULATION OF THE SPECTRUM OF GAMMA RADIATION			
4. DESCRIPTIVE NOTES (Type of report and inclusive dates) Final: September 1966 - December 1967			
5. AUTHOR(S) (First name, middle initial, last name) E. E. Morris and A. B. Chilton			
6. REPORT DATE December 1967		7a. TOTAL NO. OF PAGES 62	7b. NO. OF REFS 8
8a. CONTRACT OR GRANT NO. N0022866C0311		9a. ORIGINATOR'S REPORT NUMBER(S) Nuclear Radiation Shielding Studies Report No. 6	
b. PROJECT NO. OCD Work Unit 1112C		9b. OTHER REPORT NO(S) (Any other numbers that may be assigned this report) NRSS 6; NRDL TRC-68-6	
c.			
d.			
10. DISTRIBUTION STATEMENT This document has been approved for public release and sale; its distribution is unlimited.			
11. SUPPLEMENTARY NOTES		12. SPONSORING MILITARY ACTIVITY Office of Civil Defense Department of the Army Washington, D. C.	
13. ABSTRACT <u>Collimator, gamma rays, radiation, radioisotope, shielding</u> A Monte Carlo calculation of the energy spectrum emitted by a collimated, Co-60 source is reported. The collimator assumed is very similar to one currently being used in experimental shielding studies at the University of Illinois. Radiation emerging from the collimator is classified into 13 equal-length energy intervals between 0.1 and 1.4 MeV, and into 3 direction intervals for angles relative to the collimator axis between 0° and 90°. Comparisons are made with experimental and theoretical work reported by others.			

DD FORM 1473 (PAGE 1)

S/N 0101-807-6801

Security Classification